A chromatin-based mechanism controls differential regulation of the cytochrome P450 gene *Cyp24a1* in renal and non-renal tissues

Received for publication, July 11, 2019, and in revised form, August 8, 2019 Published, Papers in Press, August 22, 2019, DOI 10.1074/jbc.RA119.010173

Mark B. Meyer[‡1], Seong Min Lee[‡1], Alex H. Carlson[‡], Nancy A. Benkusky[‡], Martin Kaufmann[§¶], Glenville Jones[§], and J. Wesley Pike[‡2]

From the [‡]Department of Biochemistry, University of Wisconsin, Madison, Wisconsin 53706 and the Departments of [§]Biomedical and Molecular Sciences and [¶]Surgery, Queens University, Kingston, Ontario K7L 3N6, Canada

Edited by Joel M. Gottesfeld

Cytochrome P450 family 27 subfamily B member 1 (CYP27B1) and CYP24A1 function to maintain physiological levels of 1,25-dihydroxyvitamin D_3 ($1,25(OH)_2D_3$) in the kidney. Renal *Cyp27b1* and *Cyp24a1* expression levels are transcriptionally regulated in a highly reciprocal manner by parathyroid hormone (PTH), fibroblast growth factor 23 (FGF23), and $1,25(OH)_2D_3$. In contrast, *Cyp24a1* regulation in nonrenal target cells (NRTCs) is limited to induction by $1,25(OH)_2D_3$. Herein, we used ChIP-Seq analyses of mouse tissues to identify regulatory regions within the *Cyp24a1* gene locus. We found an extended region downstream of *Cyp24a1* containing a cluster of sites, termed C24-DS1, binding PTH-sensitive cAMP-responsive element–binding protein (CREB) and a cluster termed C24-DS2 binding the vitamin D receptor (VDR). VDR-occupied sites were present in both the kidney and NRTCs, but pCREB sites were occupied only in the kidney. We deleted each segment in the mouse and observed that although the overt phenotypes of both cluster deletions were unremarkable, RNA analysis in the C24-DS1–deleted strain revealed a loss of basal renal *Cyp24a1* expression, total resistance to FGF23 and PTH regulation, and secondary suppression of renal *Cyp27b1*; $1,25(OH)_2D_3$ induction remained unaffected in all tissues. In contrast, loss of the VDR cluster in the C24-DS2–deleted strain did not affect $1,25(OH)_2D_3$ induction of renal *Cyp24a1* expression yet reduced but did not eliminate *Cyp24a1* responses in NRTCs. We conclude that a chromatin-based mechanism differentially regulates *Cyp24a1* in the kidney and NRTCs and is essential for the specific functions of *Cyp24a1* in these two tissue types.

Vitamin D undergoes final bioactivation in the kidney via *Cyp27b1*-mediated 1α-hydroxylation to 1,25-dihydroxyvitamin D_3 ($1,25(OH)_2D_3$),[3] the hormonal form of the vitamin (1). Whereas $1,25(OH)_2D_3$ arises exclusively from *Cyp27b1* activity, the actual blood levels of $1,25(OH)_2D_3$ are also strongly influenced by the catabolic activity of renal CYP24A1 (2, 3). This second enzyme is active in higher concentrations than CYP27B1 in kidney mitochondria and is responsible for the degradation of both $25(OH)D_3$ and $1,25(OH)_2D_3$ to the initial intermediates $24,25(OH)_2D_3$ and $1,24,25(OH)_3D_3$, respectively. The same enzyme then performs further multistep catabolism of each of these products to specific acids, which leave the body through bile (4, 5). Whereas C24-hydroxylation is the preferred catabolic route in humans and rodents, CYP24A1 can also C23-hydroxylate $25(OH)D_3$ and $1,25(OH)_2D_3$, which culminate in terminal 26,23-lactone products; both pathways predominate in the opossum and guinea pig. New metabolite profiling methods based on LC-tandem MS are now able to detect a range of serum metabolites formed by CYP24A1, including $24,25(OH)_2D_3$, $1,24,25(OH)_3D_3$, and $25(OH)D_3$-26,23-lactone. It is questionable whether any of these metabolites are biologically active, although recent studies by St-Arnaud and colleagues (6) have suggested that $24,25(OH)_2D_3$ may act as an allosteric activator of FAM57B2 that is involved in the synthesis of lactosylceramide, providing a potential mechanism for an early hypothesized role for $24,25(OH)_2D_3$ in bone fracture healing. $1,24,25(OH)_3D_3$ is also of particular interest because recent estimates of its circulating level in mice suggest that this metabolite might contribute to the net biological activity of vitamin D_3 (7–10).

In nonrenal vitamin D target cells, inactivation of $1,25(OH)_2D_3$ by CYP24A1 likely predominates over that of $25(OH)D_3$; thus, the degradation of endocrine $1,25(OH)_2D_3$ as

This work was supported by NIDDK, National Institutes of Health, Grants R01-DK072281 and R01-DK117475 (to J. W. P.), University of Wisconsin Carbone Cancer Center Support Grant P30, and the Department of Biochemistry, University of Wisconsin (Madison, WI). The authors declare that they have no conflicts of interest with the contents of this article. The content is solely the responsibility of the authors and does not necessarily represent the official views of the National Institutes of Health.

This article was selected as one of our Editors' Picks.

All human and mouse kidney ChIP-Seq data have been deposited in the Gene Expression Omnibus under accession codes GSE129585 and GSE133025.

[1] Both authors contributed equally to this work.

[2] To whom correspondence should be addressed: Dept. of Biochemistry, University of Wisconsin-Madison, Hector F. DeLuca Biochemistry Laboratories, Rm. 543D, 433 Babcock Dr., Madison, WI 53706. Tel.: 608-262-8229; E-mail: jpike@wisc.edu.

[3] The abbreviations used are: $1,25(OH)_2D_3$, 1,25-dihydroxyvitamin D_3; FGF23, fibroblast growth factor 23; PTH, parathyroid hormone; TPTG, thyroparathyroid gland(s); NRTC, non-renal target cell; Ca, calcium; P, phosphate; CREB, cAMP-response element–binding protein; pCREB, phosphorylated CREB; Cyp24-DS1, *Cyp24a1* downstream deletion 1; Cyp24-DS2, *Cyp24a1* downstream deletion 2; qPCR, quantitative PCR; H3K4me1, monomethylated histone H3 Lys-4; H3K27ac, acetylated histone H3 Lys-27; H3K36me3, trimethylated histone H3 Lys-36; H3K9ac, acetylated histone H3 Lys-9; bw, body weight; BMD, bone mineral density; ANOVA, analysis of variance; VDR, vitamin D receptor; ROF, retention-of-function; LOF, loss-of-function; HET, heterozygous.

well as hormone potentially produced in these cells via local *Cyp27b1* expression may impact $1,25(OH)_2D_3$'s ability to control cell-specific biological actions via set point modification. The renal function of CYP24A1, however, is highlighted in the *Cyp24a1*-null mouse, wherein the loss of this enzyme's actions leads to an initial elevation in the circulating levels of $25(OH)D_3$ and $1,25(OH)_2D_3$, although secondary homeostatic events appear to down-regulate *Cyp27b1* expression in response to the reduction in $1,25(OH)_2D_3$ turnover (11, 12). The critical role of *Cyp24a1* was strongly reinforced more recently in humans with idiopathic infantile hypercalcemia, where, due to mutation in the gene, a defective CYP24A1 protein fails to degrade $1,25(OH)_2D_3$, leading to hypercalcemia and kidney disease (13). These patients exhibit significantly reduced serum $24,25(OH)_2D_3$ and elevated $25(OH)D_3/24,25(OH)_2D_3$ ratios. This observation has been recapitulated in the *Cyp24a1*-null mouse, confirming that serum vitamin D metabolite profiles serve as an effective biomarker of *Cyp24a1* expression and enzymatic activity *in vivo*.

The *Cyp24a1* gene is regulated in the kidney by the same hormones that control *Cyp27b1* expression, albeit in a reciprocal fashion (1). Thus, whereas PTH induces *Cyp27b1* expression, it strongly suppresses *Cyp24a1*; FGF23 and $1,25(OH)_2D_3$, on the other hand, strongly induce renal *Cyp24a1* yet suppress renal *Cyp27b1* (7, 14, 15). This regulatory paradigm serves both to enhance the production of $1,25(OH)_2D_3$ and to suppress its degradation under conditions of reduced $1,25(OH)_2D_3$ synthesis, thereby raising circulating levels of the hormone. High levels of $1,25(OH)_2D_3$, in contrast, decrease PTH and raise FGF23 levels, collectively suppressing CYP27B1-mediated production of $1,25(OH)_2D_3$ while increasing CYP24A1-directed degradation. Thus, reciprocal regulation of *Cyp27b1* and *Cyp24a1* in the kidney coordinately functions to raise or lower $1,25(OH)_2D_3$ levels to maintain physiologically appropriate concentrations of the hormone and thus to sustain normal extracellular mineral homeostasis (16). This reciprocal regulation does not occur in nonrenal target cells (NRTCs), however, where *Cyp24a1* is solely up-regulated by $1,25(OH)_2D_3$, potentially distancing the actions of the mineral-regulating hormones PTH and FGF23 on *Cyp24a1* expression in the kidney from those that regulate its actions in peripheral target tissues (7). Accordingly, whereas CYP27B1 is necessary for $1,25(OH)_2D_3$ production, CYP24A1 contributes to the adaptive vitamin D metabolism that controls blood $1,25(OH)_2D_3$ levels relevant to the maintenance of mineral homeostasis.

Early studies of the *Cyp24a1* gene revealed the presence of two vitamin D response elements active in mediating the response to $1,25(OH)_2D_3$ (17–22). This activity was present in virtually all cell types, including the kidney. More recently, however, we have shown using unbiased ChIP-chip and ChIP-Seq analyses that the regulation of *Cyp24a1* by $1,25(OH)_2D_3$ is also mediated by a cluster of intergenic components located downstream of the gene in both mouse and human nonrenal cells that contain functionally active vitamin D response elements, which bind the VDR upon $1,25(OH)_2D_3$ activation (23). Mechanisms that mediate both PTH and FGF23 actions in the kidney are unclear, however (7, 24–26). Finally, it is also worth noting that whereas $1,25(OH)_2D_3$, PTH, and FGF23 are primary regulators, other hormones, cytokines, and systemic components as well as intracellular chromatin coregulatory factors also modulate *Cyp24a1* expression (27–32).

Our previously reported studies revealed a unique regulatory module in the mouse kidney that is essential for the novel regulation of *Cyp27b1* by PTH, FGF23, and $1,25(OH)_2D_3$ *in vivo* (7, 26). Given the reciprocal nature of *Cyp24a1* regulation in the kidney by these same hormones together with the general absence of regulation by PTH and FGF23 in NRTCs, we initiated studies herein aimed at illuminating the underlying genomic basis for this differential regulation using both ChIP-Seq analyses and CRISPR/Cas9 gene editing methods. Our results identify a genomic mechanism in mice through which the differential expression of *Cyp24a1* occurs in the kidney and in NRTCs and highlight the role of this regulation as a primary determinant of the separate functions of *Cyp24a1* in vitamin D metabolism.

Results

Differential regulation of Cyp24a1 by PTH, FGF23, and $1,25(OH)_2D_3$ in the kidney and in NRTCs

The results in Fig. 1*A* demonstrate that *Cyp24a1* expression in the kidney is up-regulated in response to a single time- and dose-optimized injection of FGF23 or $1,25(OH)_2D_3$ in the mouse and suppressed by a similar injection of PTH, a regulatory pattern that is the reciprocal of that seen for *Cyp27b1* in the same tissue (7, 26). This control in NRTCs is limited to up-regulation by $1,25(OH)_2D_3$, however, demonstrating a collective differential regulatory response to these hormones in nonrenal tissues. It is also worth noting that the basal expression of *Cyp24a1* in the kidney is much higher than that seen in NRTCs, an observation that is now well-established. Indeed, in some NRTC tissues, basal expression levels are almost undetectable (15). The underlying determinants of elevated *Cyp24a1* expression in the kidney are not fully understood, although it is likely that the circulating levels of PTH, FGF23, and perhaps $1,25(OH)_2D_3$ contribute to this basal expression (15). Regardless of this, the differential regulation of *Cyp24a1* with respect to PTH and FGF23 in NRTCs is unique. Because some of these tissues contain mediators for both PTH and FGF23 action, it seemed unlikely that the lack of response was due to the absence of appropriate signaling pathways.

PTH, FGF23, and $1,25(OH)_2D_3$ regulate Cyp24a1 expression via transcription

Although the actions of $1,25(OH)_2D_3$ on *Cyp24a1* expression as seen in Fig. 1*A* are known to be transcriptional in nature (7, 21), the underlying mechanisms responsible for PTH suppression and FGF23 induction have been unclear. Thus, for example, it has been suggested that PTH suppression of *Cyp24a1* expression is mediated via a post-transcriptional mechanism, whereas modulation of the gene by FGF23 is entirely unknown (25, 33). We therefore conducted a ChIP-Seq analysis of the mouse genome, focusing entirely on the ability of the three hormones to alter the content of the histone mark H3K36me3 directly at the *Cyp24a1* locus. This mark has generally been linked mechanistically to levels of transcriptional elongation

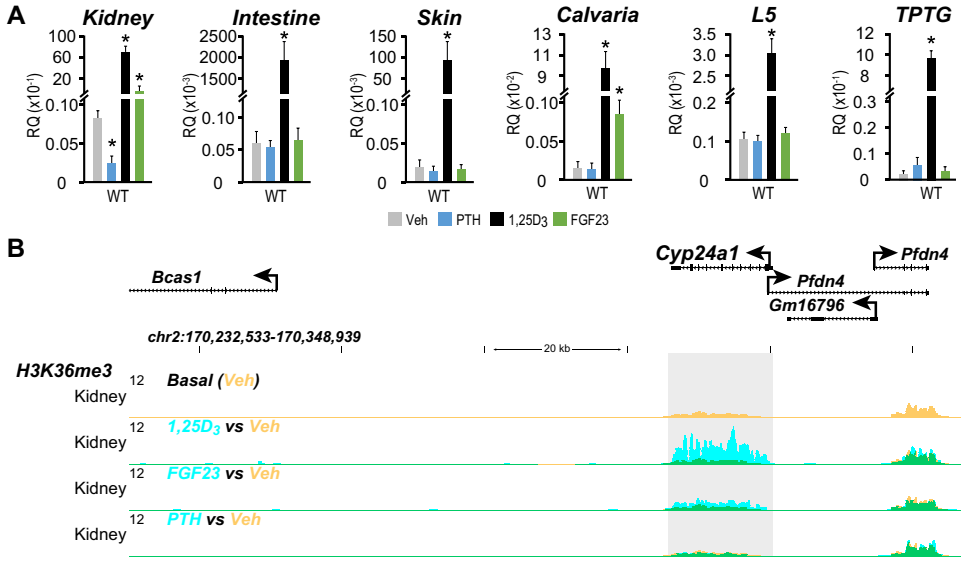

Figure 1. Transcriptional regulation of *Cyp24a1* in kidney and nonrenal target cells. *A*, gene expression of *Cyp24a1* after treatment in 8–9-week-old C57BL/6 WT mice with ethanol/PBS vehicle (*Veh*, *gray*, $n = 6$), 230 ng/g bw PTH for 1 h (*PTH*, *blue*, $n = 6$), 10 ng/g bw $1,25(OH)_2D_3$ (*1,25D$_3$*, *black*, $n = 6$) for 6 h, or 50 ng/g bw FGF23 for 3 h (*FGF23*, *green*, $n = 6$) examined in kidney, intestine, skin, calvaria, L5 vertebrae, and TPTG. Data are displayed as relative quantitation (*RQ*, mean ± S.E.) compared with *Gapdh*. *, $p < 0.05$ paired *t* test: treatment *versus* vehicle. *B*, overlaid ChIP-Seq data tracks for H3K36me3 from mouse kidney displayed as either basal or vehicle (*yellow*, $n = 3$) or treated (*blue*, $n = 3$) with $1,25(OH)_2D_3$, FGF23, or PTH as indicated with concentrations used in *A* with a treatment time of 1 h. Overlapping track data appear as *green*. Regions of interest are *highlighted* in *light gray boxes*. Genomic location and scale are indicated (*top*), and maximum height of tag sequence density for each data track is indicated on the *y axis* (*top left* of each track, normalized to input and 10^7 tags). Gene transcriptional direction is indicated by an *arrow*, and exons are indicated by *boxes*.

across most genetic loci (34). As can be seen in Fig. 1*B*, residual H3K36me3 enrichment was present exclusively within the *Cyp24a1* transcription unit in the kidney of WT mice, as predicted for this chromatin modification. Importantly, however, a 1-h treatment of each of the three hormones resulted in a striking increase in the histone mark in response to $1,25(OH)_2D_3$ and FGF23 (*blue*) and a modest suppression in response to PTH (*yellow*). Although these data do not prove that PTH and FGF23 operate at the transcriptional level, they certainly support the idea that, like $1,25(OH)_2D_3$, these hormones act directly to influence the selective output of *Cyp24a1* transcripts. As can also be seen in Fig. 1*B*, no changes in H3K36me3 density were observed at adjacent *Pfdn4*, where the transcript for this gene in the kidney is generated, or downstream of the gene at *Bcas1*, which is not transcribed (data not shown).

ChIP-Seq analysis reveals sites of VDR and pCREB binding at the Cyp24a1 gene locus in the kidney that are restricted in NRTCs to those that bind the VDR

Our preliminary examination of the *CYP24A1* gene in several mouse and human nonrenal cell lines using ChIP-Seq analysis suggested the $1,25(OH)_2D_3$-inducible presence of the VDR at novel sites located in the intergenic region downstream of *CYP24A1* as well as immediately upstream of the *Cyp24a1* promoter (23, 35, 36). Using this same technique in mouse tissues, the results in Fig. 2*A* confirm that 1 h after $1,25(OH)_2D_3$ injection, the VDR was present at various densities in these same downstream (termed herein *Cyp24a1*-downstream 2 (C24-DS2)) and upstream (termed *Cyp24a1* promoter–proximal 1 (C24-PP1)) sites in isolated nonrenal mesenchymal cells, small intestinal tissue, thyroparathyroid glands (TPTG), and bone marrow cells and also in kidney tissue. Importantly, ChIP-Seq analysis of the kidney also revealed the modest presence of phosphorylated CREB (pCREB), a major protein kinase A/PTH transcription factor target, at several sites in C24-DS2 but most strongly at three additional novel sites in a region (termed Cyp24a1-downstream 1 (C24-DS1)) located more proximal to the 3′ end of the *Cyp24a1* gene yet outside the VDR binding cluster itself. pCREB was apparent in the C24-PP1 region of *Cyp24a1* as well. As noted earlier, *Pfdn4* was not regulated by any of the three hormones here or in NRTCs and is therefore not a target gene. A similar analysis 1 h after PTH injection revealed a modest effect to reduce pCREB (*yellow*) levels within C24-DS1 that could represent a mechanistic determinant of PTH suppression, although additional studies will be required to firmly establish this finding. Interestingly, as documented in Fig. 2*B*, neither residual nor inducible pCREB was present across the entire region of C24-DS1 or in C24-PP1 in mesenchymal stem cells (*MSC*) or peripheral blood monocytes (*pBMCs*) or in any other NRTCs we examined (data not shown). These results suggest that whereas VDR is capable of occupying sites and mediating activity at the *Cyp24a1* gene in both the kidney and in representative NRTCs, the absence of pCREB binding and perhaps other factor activities likely restrict the effects of PTH and FGF23 in NRTCs.

H3K4me1 and H3K9ac enrichment co-localizes with both VDR- and pCREB-occupied sites at the Cyp24a1 gene locus in the kidney but is selectively absent at unoccupied pCREB sites in the intestine

To assess whether sites of VDR- and pCREB-binding activity were contained within active enhancers, we conducted a further ChIP-Seq analysis of H3K4me1 and of H3K9ac across the *Cyp24a1* gene locus; the former histone modification represents a classic epigenetic enhancer signature mark, whereas the latter represents an epigenetic mark that is frequently indica-

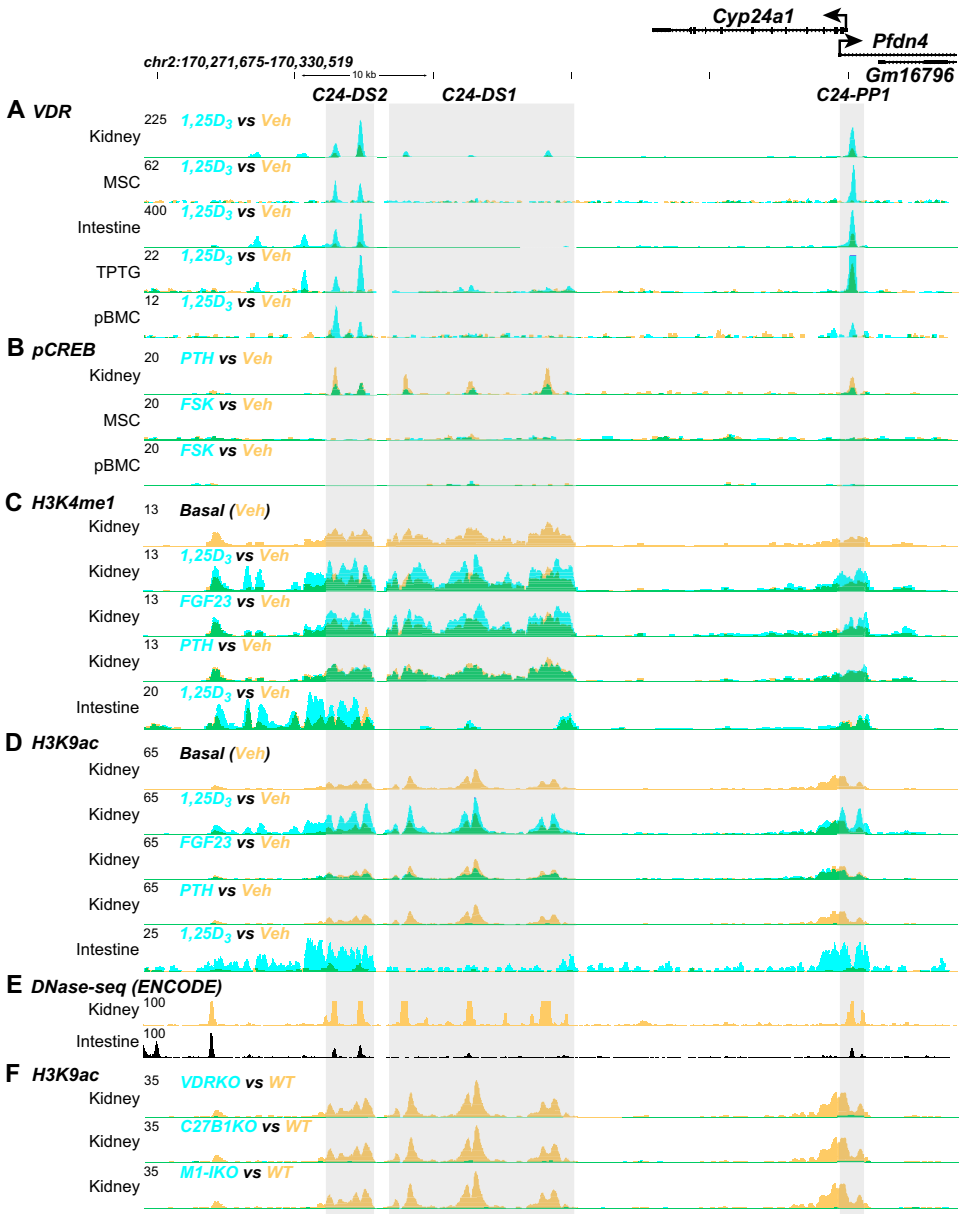

Figure 2. ChIP-Seq analysis displays kidney-specific regulation at the *Cyp24a1* gene locus. *A–D*, overlaid ChIP-Seq data tracks for VDR (*A*), pCREB (*B*), H3K4me1 (*C*), and H3K9ac (*D*) from mouse kidney, bone marrow–derived mesenchymal stem cells (*MSC*), intestine, TPTG, or peripheral blood monocytes (*pBMC*) displayed as either basal or vehicle (*yellow*, $n = 3$) or treated (*blue*, $n = 3$) with PTH, forskolin (*FSK*), 1,25$(OH)_2D_3$, or FGF23, as indicated. *E*, DNase-Seq data from the ENCODE project for kidney and intestine. *F*, H3K9ac data in VDRKO (*blue*), Cyp27b1KO mice (C27B1KO, *blue*), or M1-IKO (*blue*) *versus* WT (*yellow*). Overlapping track data appear as *green*. Regions of interest are *highlighted* in *light gray boxes* denoted as C24-DS1, C24-DS2, and C24-PP1. Genomic location and scale are indicated (*top*), and maximum height of tag sequence density for each data track is indicated on the *y axis* (*top left* of each track, normalized to input and 10^7 tags). Gene transcriptional direction is indicated by an *arrow*, and exons are indicated by *boxes*.

tive of altered enhancer activity (34, 37). Accordingly, mice were treated with either vehicle, PTH, FGF23, or 1,25$(OH)_2D_3$ for 1 h and then subjected to ChIP-Seq analysis as in the earlier studies of H3K36me3. As seen in Fig. 2*C*, basal enrichment of the H3K4me1 mark was evident not only at C24-PP1 but also at a number of broad sites that align directly with sites that retain VDR (C24-DS2) and/or pCREB (C24-DS1) across the intergenic segment located downstream of the *Cyp24a1* locus. Both 1,25$(OH)_2D_3$ and FGF23 modestly induce H3K4me1 densities at each of these potential enhancer regions, although the suppressor PTH is without effect on this mark. Importantly, whereas significant H3K4me1 enrichment aligned within the VDR-binding regions in the intestine, no such enrichment was evident within the C24-DS1 segment that binds pCREB exclusively in the kidney. As seen in Fig. 2*D*, similar basal and regulatory profiles were observed for the H3K9ac enhancer activity mark. In this case, however, whereas 1,25$(OH)_2D_3$ actively induces the H3K9ac mark, FGF23 had at best a modest effect on this modification (1,25$(OH)_2D_3$ is a much stronger inducer), whereas PTH was seen to suppress this mark strongly, demonstrating expected selectivity relative to H3K9ac. Again, however, whereas the H3K9ac mark was present and aligned with VDR occupancy and H3K4me1 enrichment in the intestine (C24-DS2) and was also seen to increase in response to

Table 1
Animal models employed

Strain/type	Phenotype	Reference
WT	None	
C24-DS1KO	Low *Cyp24a1* basal, reciprocally low *Cyp27b1* basal	This work
C24-DS2KO	*Cyp24a1* 1,25$(OH)_2D_3$-sensitive in NRTC only	This work
Cyp27b1-null	*Cyp27b1*-null, low *Cyp24a1* basal	Refs. 7 and 26
Cyp24a1-null	*Cyp24a1*-null	Ref. 11
M1-IKO	Low *Cyp27b1* basal, *Cyp27b1* PTH-insensitive	Refs. 7 and 26
M21-IKO	Low *Cyp27b1* basal, *Cyp27b1* FGF23-insensitive	Refs. 7 and 26
M1/M21-DIKO	Low *Cyp27b1* basal, *Cyp27b1* PTH/FGF23/1,25$(OH)_2D_3$-insensitive	Ref. 26

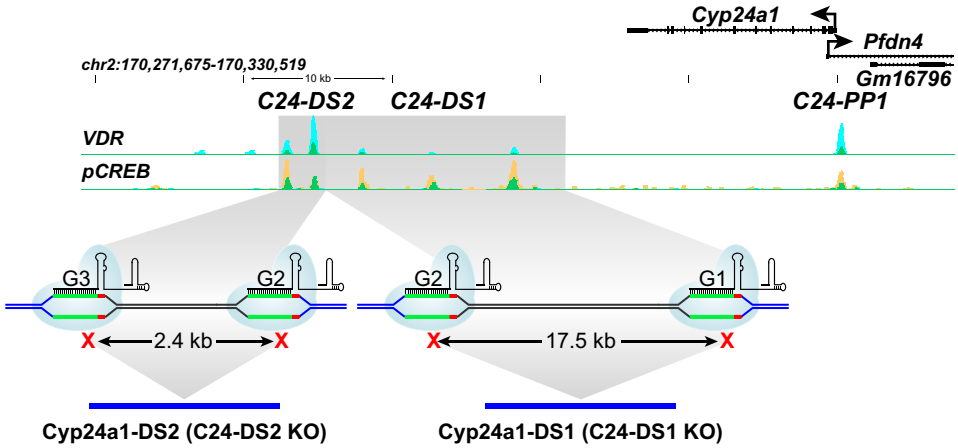

Figure 3. *Schematic representation* of the CRISPR/Cas9 deletions in the downstream regions of the *Cyp24a1* locus. VDR and pCREB ChIP-Seq data (as in Fig. 2) are shown for reference. *Highlighted regions* were excised using two CRISPR-guide RNAs each for *Cyp24a1*-DS1KO and *Cyp24a1*-DS2KO. Both regions shared a common guide RNA (*G2*).

1,25$(OH)_2D_3$, no such activity was evident across the C24-DS1 segment unable to bind pCREB. This was also true for other NRTC tissues (data not shown).

This extended downstream region also contained open chromatin sites, as identified through studies conducted by the ENCODE Consortium in both kidney and intestine. In these experiments, DHS analysis of the tissues of 8-week-old mice revealed the presence of well-defined open chromatin sites that aligned directly with both VDR- and pCREB-bound enhancers (C24-DS2 and C24-DS1, respectively) in the kidney but were restricted exclusively to VDR C24-DS2 sites in the intestine (Fig. 2*E*). Finally, we conducted ChIP-Seq analysis of H3K9ac in the kidneys of *Vdr*- and *Cyp27b1*-null mice, which have highly suppressed *Cyp24a1* expression levels due to highly elevated PTH and strongly suppressed FGF23 concentrations in the blood (7, 15, 26), and in M1-IKO mice where elevated PTH and lowered FGF23 parameters also exist, although for different mechanistic reasons (see Table 1) (7, 26). As can be seen in Fig. 2*F*, whereas H3K9ac enrichment was present in WT mice, there was no evidence of H3K9ac activity at sites across the entire *Cyp24a1* gene locus in any of these mouse strains. These data not only support the relevance of the H3K9ac mark for *Cyp24a1* activity but also demonstrate that despite the presence (M1-IKO mice) or absence (*Cyp27b1*-null mice) of 1,25$(OH)_2D_3$ or the absence of 1,25$(OH)_2D_3$ activity (*Vdr*-null mice), high PTH and low FGF23 levels prevent the expression and regulation of *Cyp24a1*. In addition, these overall observations indicate that the factor that mediates FGF23 activity is likely to bind to the same region to which pCREB alone is bound.

Establishing the functional role of the DS1 regulatory region

The large downstream regulatory domain for *Cyp24a1* that contains multiple components that generally favor either VDR (C24-DS2) or pCREB (C24-DS1) binding is clearly complex in its linear arrangement, spanning almost 30 kb of DNA. In addition, whereas the distinction between the numerous VDR and pCREB binding sites is clear, particularly in the kidney *versus* other NRTCs, it is also evident that modest transcription factor overlap may exist at a subset of these sites in the kidney. Given this complexity, we employed a CRISPR/Cas9 gene editing approach as documented in Fig. 3 and deleted either 17.5 kb of DNA containing the three dominant pCREB binding sites or 2.4 kb containing the two major sites of VDR binding and created two mutant mouse strains designated Cyp24-DS1KO (C24-DS1KO, 17.5-kb deletion) and Cyp24-DS2KO (C24-DS2KO, 2.4-kb deletion), respectively (7). Male and female C24-DS1KO mice appeared normal in size, weight, and appearance as compared with WT littermate controls, and their skeletons exhibited normal whole-body, femur, and spine bone mineral densities (BMDs), as documented in Table 2. Interestingly, whereas both blood calcium (Ca) and phosphate (P) levels were also comparable with controls, providing the basis for the normal skeletal BMDs that were observed, PTH levels were modestly suppressed, whereas FGF23 levels were somewhat elevated (Table 3). These results suggested that although mineral homeostasis was normal, minor hormonal adaptations might accommodate the maintenance of Ca and P levels within the normal range. Based upon these initial observations, we isolated kidney RNA and examined the overall expression of *Cyp24a1*. As can

Table 2
Bone mineral densities and body weights ($n = 6–13$)

	Sex	WT	DS1
Whole body (g/cm^2)	Female	0.045 ± 0.001	0.045 ± 0.001
	Male	0.049 ± 0.001	0.049 ± 0.001
Femur (g/cm^2)	Female	0.060 ± 0.001	0.060 ± 0.001
	Male	0.074 ± 0.001	0.074 ± 0.001
Spine (g/cm^2)	Female	0.058 ± 0.002	0.056 ± 0.001
	Male	0.062 ± 0.001	0.061 ± 0.001
Body weight (g)	Female	19.8 ± 0.5	19.5 ± 0.2
	Male	24.6 ± 0.3	24.4 ± 0.4

Table 3
Systemic factor analyses ($n = 13$)
*, $p < 0.05$ *versus* WT littermates.

Factor	WT	DS1
Calcium (mg/dl)	10.7 ± 0.2	10.9 ± 0.2
Phosphate (mM)	2.7 ± 0.1	2.6 ± 0.1
PTH (pg/ml)	48.2 ± 1.4	39.8 ± 0.3*
FGF23 (pg/ml)	244.4 ± 10.2	319.7 ± 13.0*

be seen in Fig. 4 (*A–C*), basal *Cyp24a1* expression in vehicle-treated mice was dramatically reduced in the kidney, whereas *Cyp24a1* response to a single injection of either FGF23 (Fig. 4*A*) or PTH (Fig. 4*B*) was fully abrogated relative to similarly treated littermate controls. These results support the hypothesis that this large regulatory segment in normal mice likely mediates both PTH and FGF23 modulation. Interestingly, the noted reduction in *Cyp24a1* expression in the kidneys of C24-DS1KO mice was also accompanied by a secondary reduction in *Cyp27b1* expression, as seen in Fig. 4*A*, likely the result of homeostatic adaptation prompted by decreased PTH and increased FGF23 levels, as discussed previously (Table 2). This coordinated secondary reduction in *Cyp27b1* is analogous to that seen for *Cyp24a1* when *Cyp27b1* expression is reduced in *Cyp27b1*-null, M1-IKO, and M1/M21-DIKO mice as a result of elevated PTH and reduced FGF23 levels (see Table 4) (7, 26) and appears to be a hallmark of the reciprocal regulation of these two genes.

Importantly, treatment of the mutant mice with $1,25(OH)_2D_3$ resulted in a strong up-regulation of *Cyp24a1* expression in the kidney (Fig. 4*C*), although this up-regulation was slightly compromised relative to WT mice. It is worth noting, however, that WT -fold induction by $1,25(OH)_2D_3$ was ~46-fold above baseline, whereas in the C24-DS1 mice, it was 740-fold. Because the basal expression of *Cyp24a1* in C24-DS1KO mice is strongly reduced, it is difficult to ascertain at this level of resolution whether the decreased net response to $1,25(OH)_2D_3$ is due to the absence of potentially overlapping sites of weak VDR binding in C24-DS1 or to the absence of regulatory sites responsible for basal *Cyp24a1* expression in C24-DS1 that might influence the activity of $1,25(OH)_2D_3$. It seems unlikely, however, that the reduced response to $1,25(OH)_2D_3$ is due to changes in VDR DNA-binding activity present in the C24-DS2 segment, because *Vdr* concentrations at the level of RNA remain unaltered.

In contrast, examination of *Cyp24a1* expression in multiple NRTCs, including intestine, bone, spleen, thymus, and skin, in the C24-DS1KO mouse (Fig. 4*D*) revealed that neither basal nor $1,25(OH)_2D_3$ induction was compromised in any of these tissues with the exception of the TPTG, which, like the kidney,

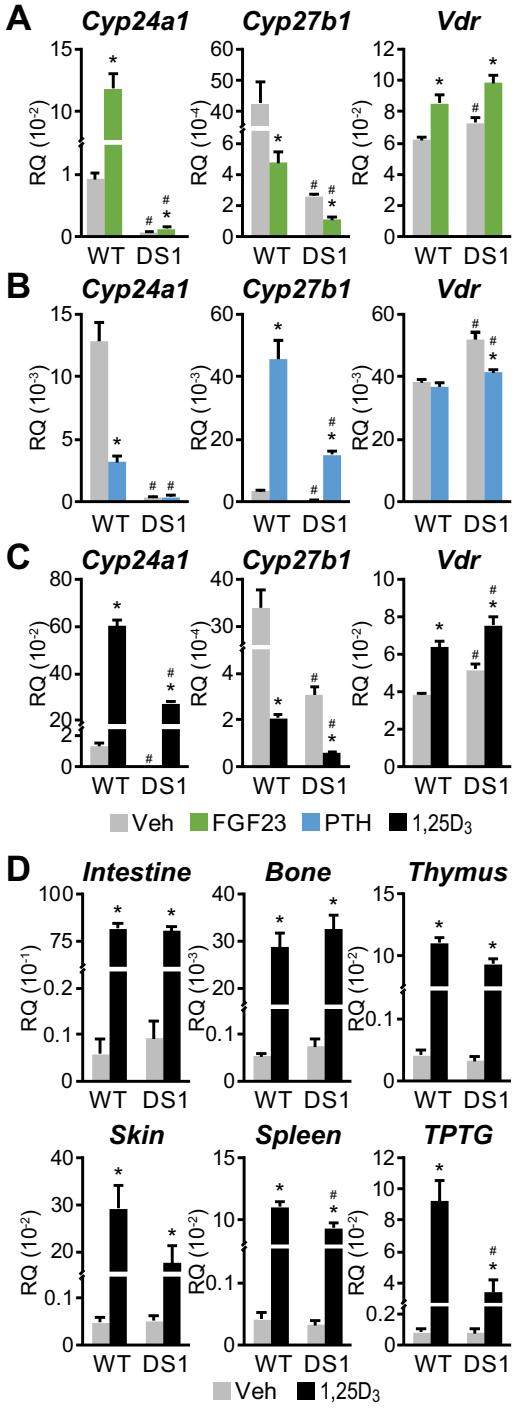

Figure 4. Transcriptional regulation of *Cyp24a1* in Cyp24-DS1KO mice. *A–C*, expression of the genes indicated after treatment in 8–9-week-old Cyp24-DS1KO mice (DS1) and their WT littermates (*WT*) with ethanol/PBS vehicle (*Veh*, *gray*, $n = 6–10$), 50 ng/g bw FGF23 for 3 h (FGF23, *green*, $n = 6$), 230 ng/g bw PTH for 1 h (*PTH*, *blue*, $n = 8$), or 10 ng/g bw $1,25(OH)_2D_3$ (*1,25D$_3$*, *black*, $n = 9$) for 6 h was examined in kidney. *D*, gene expression of *Cyp24a1* after treatment in 8–9-week-old DS1 mice (*DS1*) and their WT littermates (*WT*) with ethanol vehicle (*Veh*, gray, $n = 8–9$), or 10 ng/g bw $1,25(OH)_2D_3$ (*1,25D$_3$*, *black*, $n = 9$) for 6 h was examined in nonrenal tissues as indicated. Data are displayed as relative quantitation (*RQ*, mean ± S.E. (*error bars*)) compared with *Gapdh*. *, $p < 0.05$, paired *t* test: treatment *versus* vehicle. #, $p < 0.05$, paired *t* test: DS1 *versus* WT received the same treatment.

exhibited a reduced response to the hormone. Finally, it is interesting to note with respect to C24-DS1KO mice that because FGF23 induces whereas PTH suppresses *Cyp24a1*, the striking

Table 4
Vitamin D_3 metabolite analyses ($n = 6–8$)
ND, not determined; *, $p < 0.05$ *versus* WT littermates.

Metabolite	WT	DS1	WT	DS2
$25(OH)D_3$ (ng/ml)	14.8 ± 1.0	51.0 ± 3.4*	16.8 ± 0.3	15.3 ± 0.9
$24,25(OH)_2D_3$ (ng/ml)	7.8 ± 0.8	26.5 ± 4.5*	8.1 ± 0.7	7.0 ± 0.3
$25(OH)D_3/24,25(OH)_2D_3$ ratio	1.9 ± 0.3	2.0 ± 0.5	2.2 ± 0.4	2.2 ± 0.2
$25(OH)D_3$-26,23-lactone (ng/ml)	3.1 ± 0.2	1.1 ± 0.1*	4.8 ± 0.2	4.4 ± 0.3
$25(OH)D_3/25(OH)D_3$-26,23-lactone ratio	4.9 ± 0.9	47.3 ± 12.4*	3.5 ± 0.5	3.5 ± 0.4
$1,25(OH)_2D_3$ (pg/ml)	24.6 ± 2.4	26.8 ± 1.4	21.2 ± 2.2	18.8 ± 1.3
$1,24,25(OH)_3D_3$ (pg/ml)	70.9 ± 2.9	44.8 ± 3.6*	68.8 ± 3.2	66.8 ± 4.2

loss of basal expression of *Cyp24a1* in these mice may be due entirely to the loss of responsivity to FGF23 induction. Because PTH is a suppressor, it is clear that loss of this response would result in derepression, an effect opposite that of FGF23. This interpretation would point to FGF23 as the dominant physiological regulator of basal *Cyp24a1* expression in the kidney.

Vitamin D metabolism in C24-DS1KO mice

Based upon the systemic phenotype associated with the C24-DS1 mutation and the features of *Cyp24a1* expression in the kidney and in NRTCs, we assessed in an additional examination whether the reduction in both *Cyp24a1* and *Cyp27b1* resulted in an aberrant level of $1,25(OH)_2D_3$ and/or other vitamin D metabolites that comprise a vitamin D metabolite panel. As can be seen in Table 4, circulating levels of the $1,25(OH)_2D_3$ hormone were normal in C24-DS1KO mice as compared with WT littermate controls and were consistent with normal mineral levels and skeletal BMDs seen in these mice as well. Interestingly, however, a significant alteration in the level of key metabolites of vitamin D was evident in the blood of C24-DS1KO mice that clearly resulted from the reduction in *Cyp24a1* expression. Thus, in contrast to normal mice, where levels of $25(OH)D_3$ and $24,25(OH)_2D_3$ were maintained at a ratio of between 1.6 and 2.0, there was a 3–4-fold increase in the absolute amounts of both $25(OH)D_3$ and $24,25(OH)_2D_3$ coincident with a largely unchanged ratio between the two metabolites in C24-DS1KO mice. These findings support a markedly reduced catabolism of the $25(OH)D_3$ substrate and a corresponding steady-state accumulation of the initial $24,25(OH)_2D_3$ catabolic product of CYP24A1 activity. The decrease in CYP24A1 activity toward $25(OH)D_3$ was particularly reinforced by the observed reduction in $25(OH)D_3$-26,23-lactone, the metabolite arising from CYP24A1 catabolism via the $23,25(OH)_2D_3$ metabolic pathway, and by the dramatic increase in the ratio of $25(OH)D_3/25(OH)D_3$-26,23-lactone from 5 in WT mice to 47 in the C24-DS1 mouse, both consistent with reduced *Cyp24a1* expression. Clearly, while the ratio of $25(OH)D_3$ to the initial catabolic product of the $24,25(OH)_2D_3$ degradation pathway ($24,25(OH)_2D_3$) remained largely unchanged, the ratio of $25(OH)D_3$ to the terminal catabolic product of the $23,25(OH)_2D_3$ degradation pathway was strikingly increased. Finally, C24-DS1KO mice also displayed lowered $1,24,25(OH)_3D_3$ levels as compared with WT littermate controls, confirming impaired catabolism of the $1,25(OH)_2D_3$ metabolites as well. This metabolic profile is consistent with that seen in other mouse models where *Cyp24a1* levels are significantly reduced (see Table 1) (7, 26). We conclude that this mutant mouse with compromised *Cyp24a1* and reduced *Cyp27b1* expression levels exclusively in the kidney is able to maintain normal Ca and P homeostasis via a minor suppression in PTH and a modest elevation in FGF23 that significantly alters vitamin D metabolism to accommodate the maintenance of appropriate levels of $1,25(OH)_2D_3$.

The role of Cyp24a1 in the regulation of circulating 25(OH)D_3

The vitamin D metabolic profile observed in the C24-DS1KO mouse above as well as profiles of a similar nature that had emerged in earlier mutant mouse models of altered *Cyp24a1* expression suggested the possibility that in addition to its regulation of $1,25(OH)_2D_3$, *Cyp24a1* might be an important determinant of circulating $25(OH)D_3$ levels as well. To explore this idea, we plotted the blood levels of $25(OH)D_3$, $24,25(OH)_2D_3$, and $25(OH)D_3$-26,23-lactone as a function of basal renal *Cyp24a1* expression in tissues obtained from WT mice (defined as 100%) and from several of the mutant mouse strains we alluded to above that exhibited variable decreases in basal *Cyp24a1* expression levels (*Cyp24a1* expression was indicated as a percentage of the level measured in WT littermate controls). The mutant strains utilized were M1-IKO, M21-IKO, and M1/M21-DIKO mice, which exhibit resistance to PTH and/or FGF23 or $1,25(OH)_2D_3$; *Cyp27b1*-null mice, which cannot synthesize $1,25(OH)_2D_3$; and *Cyp24a1*-null mice, which cannot catabolize either $25(OH)D_3$ or $1,25(OH)_2D_3$ (phenotypes summarized in Table 1) (7, 26, 38). We used these strains specifically because, with the exception of the *Cyp24a1*-null mouse, they each contained mutations at the *Cyp27b1* locus that altered *Cyp27b1* expression and $1,25(OH)_2D_3$ production, which allowed for a common differential, homeostatic suppression of renal *Cyp24a1* expression. As can be seen in Fig. 5, declining *Cyp24a1* expression over a significant range beginning with WT levels correlated directly with modestly increasing concentrations of both $25(OH)D_3$ and the initial metabolic degradation product $24,25(OH)_2D_3$ such that the ratio of the two metabolites remained relatively constant between 1.6 and 2.0, ratios similar to that observed in the C24-DS1KO mouse (Table 4). An inflection point for *Cyp24a1* expression was observed in M21-IKO mice, however, where $24,25(OH)_2D_3$ levels began to decrease while $25(OH)D_3$ substrate levels continued to rise, resulting in a ratio of $25(OH)D_3$ to $24,25(OH)_2D_3$ above 2. The effects of further decreases in *Cyp24a1* expression were even more striking in M1-IKO, M1/M21-DIKO, and *Cyp27b1*-null mice, wherein $24,25(OH)_2D_3$ levels decreased rapidly to below the limits of detection (loss of synthesis) while $25(OH)D_3$ levels continued to rise almost exponentially (loss of catabolism); the ratio of the two metabolites also continued to

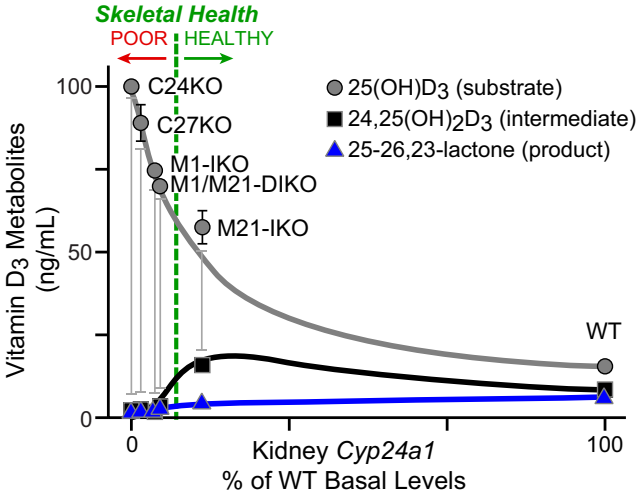

Figure 5. *Schematic representation* of *Cyp24a1* expression levels correlated to vitamin D_3 metabolites may help predict skeletal health. Shown is the percentage of *Cyp24a1* gene expression levels (*x axis*) plotted against 25(OH)D_3 (*gray circles*), 24,25(OH)$_2D_3$ (*black squares*), and 25(OH)D_3-26,23-lactone (*blue triangles*) concentrations (*y axis*) in *Cyp24a1*-null (*C24KO*), *Cyp27b1*-null (*C27KO*), M1-IKO, M1/M21-DIKO, M21-IKO, and WT littermate control (*WT*) mice. Skeletal health of the animals is depicted by a *green dashed line*. Animals to the *right* of the line are "healthy," and those to the *left* are in "poor" skeletal health relative to Ca and P levels as well as circulating concentrations of PTH, FGF23, and 1,25(OH)$_2D_3$ (6, 29). *Error bars*, S.E.

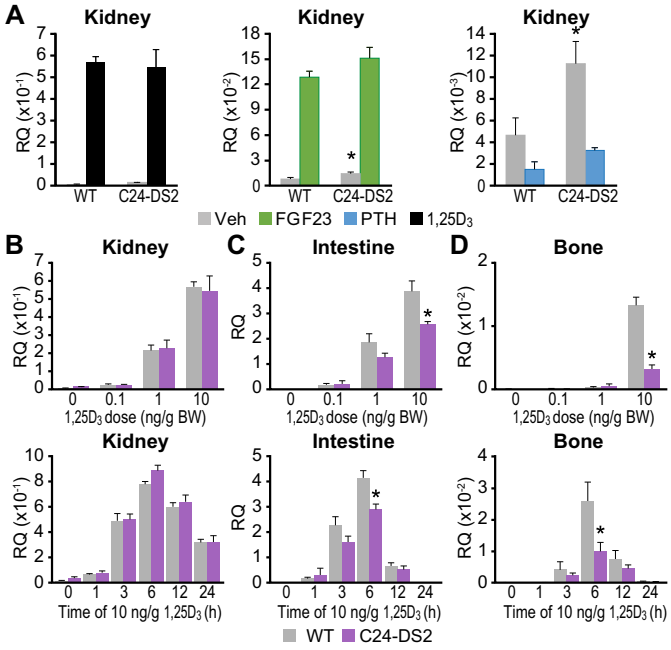

Figure 6. Transcriptional regulation of *Cyp24a1* in Cyp24-DS2KO mice. *A*, gene expression of *Cyp24a1* after treatment in 8–9-week-old Cyp24-DS2KO mice (C24-DS2) and their WT littermates (*WT*) with ethanol/PBS vehicle (*Veh*, *gray*, $n = 4–6$), 10 ng/g bw 1,25(OH)$_2D_3$ (*1,25D$_3$*, *black*, $n = 5–6$) for 6 h, 50 ng/g bw FGF23 for 3 h (*FGF23*, *green*, $n = 5–6$), or 230 ng/g bw PTH for 1 h (*PTH*, *blue*, $n = 5–6$) was examined in kidney. *B–D*, gene expression of *Cyp24a1* after treatment in 8–9-week-old Cyp24-DS2KO mice (C24-DS2) and their WT littermates (*WT*) with ethanol vehicle (*Veh*, *gray*, $n = 4$) or either the indicated amounts of 1,25(OH)$_2D_3$ (*purple*, $n = 4–5$) for 6 h (*top row*) or 10 ng/g bw 1,25(OH)$_2D_3$ (*purple*, $n = 4–5$) for the indicated periods of time (*bottom row*) was examined in kidney (*B*), intestine (*C*), or bone (*D*). Data are displayed as relative quantitation (*RQ*, mean ± S.E. (*error bars*)) compared with *Gapdh*. *, $p < 0.05$, paired *t* test: C24-DS2 *versus* WT received the same treatment.

increase as well. Finally, as illustrated in the *Cyp24a1*-null mouse (unable to synthesize 24,25(OH)$_2D_3$), 25(OH)D_3 reached a peak of over 100 ng/ml, and the ratio of 25(OH)D_3 to 24,25(OH)$_2D_3$ rose to >50. In contrast to this profile, however, the levels of the terminal degradation product 25(OH)D_3-26,23-lactone decreased in direct proportion to decreasing levels of *Cyp24a1* expression. Thus, the ratios of 25(OH)D_3/25(OH)D_3-26,23-lactone in the M1-IKO, M21-IKO, and M1/M21-DIKO mice as well as the *Cyp24a1*-null and *Cyp27b1*-null mice all increased to well above 500. The results in the *Cyp24a1*-null mouse confirm a recent similar measurement in the same mutant mouse strain, a study that also included several humans with inactivating *CYP24A1* mutations characteristic of idiopathic infantile hypercalcemia (13, 39, 40). Collectively, these results suggest that an additional role for renal *Cyp24a1* may be to modulate actively the circulating levels of 25(OH)D_3 via degradation.

Establishing the functional role of the Cyp24-DS2KO regulatory region

Having established a key function of the downstream C24-DS1 regulatory region, we turned to an assessment of the dominant downstream VDR sites located within the C24-DS2 region in C24-DS2KO mice. A peripheral examination revealed a normal size and weight as well as growth pattern in both sexes of these mutant mice relative to their WT littermate counterparts; all of the systemic parameters of these mice that we measured were also equivalent to their WT littermate controls (data not shown). In addition, all mutant mice exhibited a vitamin D metabolite profile including 1,25(OH)$_2D_3$ levels that were each consistent with that of their WT littermate controls (Table 4). These results led us to predict at best only modest effects on basal expression of *Cyp24a1* and perhaps only a modest reduction in response to 1,25(OH)$_2D_3$ in all tissues. Surprisingly, as seen in Fig. 6*A*, whereas basal expression of *Cyp24a1* was only slightly elevated above normal, this deletion had no effect on either the dose- or time-dependent induction of *Cyp24a1* by 1,25(OH)$_2D_3$ in the kidneys of these mice (Fig. 6*B*). As expected, however, *Cyp24a1* responses to both FGF23 and PTH in the kidney remained fully intact (Fig. 6*A*). Given the loss of significant VDR-binding sites within the downstream C24-DS2 region, this result suggests that 1,25(OH)$_2D_3$ action in the kidney is likely mediated exclusively via elements located near the *Cyp24a1* gene promoter (C24-PP1). Unexpectedly, however, a similar examination of *Cyp24a1* expression and regulation in intestine and bone (two NRTCs tissues) revealed that the loss of the C24-DS2 region significantly reduced the dose- and time-dependent induction of *Cyp24a1* by 1,25(OH)$_2D_3$ (Fig. 6, *C* and *D*). The sources of the residual response to 1,25(OH)$_2D_3$ in these tissues could be derived from either additional VDR binding sites located further downstream of C24-DS2 or through sites located within C24-PP1 or both, although our previous observations using bacterial artificial chromosome clone-transfected bone cells indicate that the *Cyp24a1* promoter-proximal-based mechanism is most likely (23). Whereas an effect on basal *Cyp24a1* expression in these NRTCs was not seen, an accurate assessment of the gene's basal expression remains difficult, given the low level of *Cyp24a1* expression in both of these tissues. Regardless of the source, these

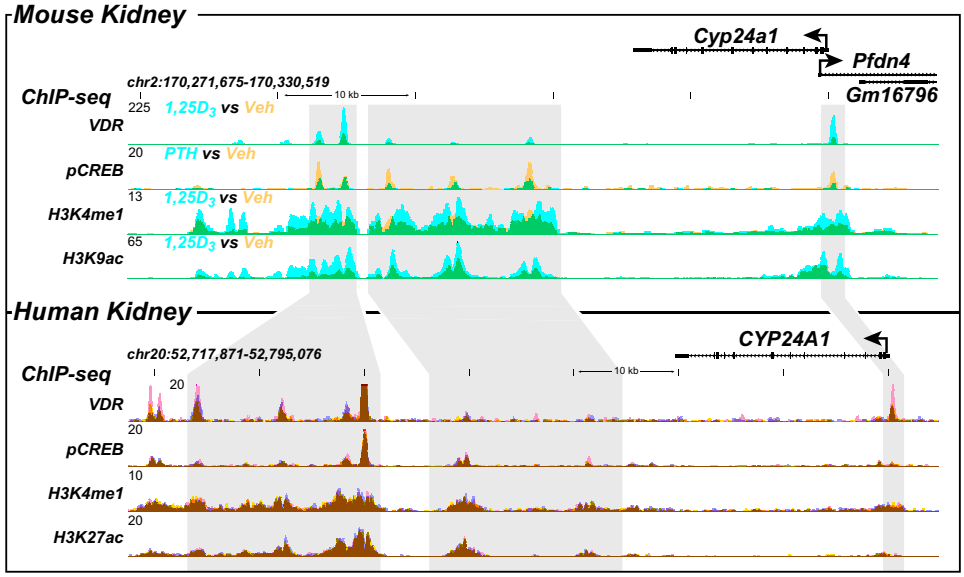

Figure 7. ChIP-Seq analysis of the human kidney reveals conserved genomic occupancy at the *CYP24A1* gene locus relative to the mouse. ChIP-Seq analysis of the mouse kidney (*top*, as in Fig. 2) was contrasted with that derived from isolated human kidney cortex. Overlaid ChIP-Seq data tracks for VDR, pCREB, H3K4me1, and H3K9ac at the *Cyp24a1* gene locus from mouse kidney (*top*) are displayed as either basal or vehicle (*yellow*, $n = 3$) or treated for 1 h with PTH or 1,25(OH)$_2$D$_3$ (*blue*, $n = 3$), as indicated. Overlapping data (vehicle and treatment) appear as *green*. *Bottom*, human kidney ChIP-Seq data for pCREB, VDR, H3K4me1, and H3K27ac at the *CYP24A1* gene locus are displayed in triplicate (*blue*, *yellow*, and *pink*; overlaps appear as *brown*). The DS1 and DS2 regions of interest are *highlighted* in *light gray boxes*, where the activity of DS2 in NRTCs was established previously (23). Genomic location and scale are indicated (*top*), and maximum height of tag sequence density for each data track is indicated on the *y axis* (*top left* of each track, normalized to input and 10^7 tags). The direction of transcription is indicated by the *arrow*, and *exons* are indicated by *boxes*.

results suggest that the deleted downstream region in the C24-DS2KO mouse contributes in a unique manner to the sensitivity of *Cyp24a1* to 1,25(OH)$_2$D$_3$-mediated up-regulation in these two NRTC tissues. We conclude from this study that the downstream VDR/pCREB regulatory region plays a unique basal but not 1,25(OH)$_2$D$_3$-inducible role for *Cyp24a1* in the kidney, yet a striking role in mediating the degree of 1,25(OH)$_2$D$_3$ response in NRTCs.

The genomic arrangement of the human CYP24A1 gene in the kidney is similar to that in the mouse kidney

Cyp24a1 is expressed in vitamin D target tissues of all species examined, although basal levels are generally much lower in NRTCs as compared with the kidney. The general regulation by 1,25(OH)$_2$D$_3$ in human cells and tissues is also similar, although informative ChIP-Seq scans of the *CYP24A1* locus aimed at 1,25(OH)$_2$D$_3$ regulation have been limited generally to human NRTC cell lines or primary cells in culture (35, 36, 41–43). Thus, ChIP-Seq analyses of the *CYP24A1* locus in human kidney tissue with a focus on regulatory components that might mediate not only 1,25(OH)$_2$D$_3$ but PTH and FGF23 action as well have not been conducted. To explore this aspect of *CYP24A1* expression relative to our current view of the mouse renal *Cyp24a1*, we obtained a donated human kidney (26) and conducted both an RNA analysis of *CYP24A1* expression and a ChIP-Seq analysis of tissue from the cortex of this organ and compared the genetic and epigenetic landscape with that from the mouse. We assessed residual VDR and pCREB occupancy as well as epigenetic enrichment of H3K4me1 and H3K27ac marks that likely represent signatures of active enhancers. *CYP24A1* expression was detected as reported previously (26). The ChIP-Seq tracks in Fig. 7 reveal that both the VDR and pCREB occupy sites near the gene's promoter; the VDR binds downstream of the gene to a subset of sites located distal to the 3′ end of the gene as well. pCREB, on the other hand, while appearing to occupy several unique sites more proximal to the 3′ end of the gene, also co-localizes strongly with virtually all of the more distal sites that bind the VDR. Importantly, each of these novel sites across this downstream locus that bind VDR and pCREB in the human kidney aligns directly with the H3K4me1 and H3K27ac marks that are indicative of the presence of active enhancers. Finally, although linear distances from the *CYP24A1* promoter in the human gene differ significantly from those seen in the mouse, the locations and arrangement of these enhancer sites are generally similar. These data in the human kidney together with previous analyses in human cell lines support the idea that the organization of the *CYP24A1* gene is highly conserved in both the mouse and human genomes. We entertain the possibility, however, that the actions of PTH, FGF23, and 1,25(OH)$_2$D$_3$ within individual enhancers may be consolidated in humans rather than uniquely dispersed across individual enhancers as in the mouse.

Discussion

Cyp24a1 is differentially regulated in mouse tissues such that the gene is highly modulated in the kidney by PTH, FGF23, and 1,25(OH)$_2$D$_3$, whereas in NRTCs, such as skin, immune cells, bone, and intestine, its regulation is restricted to that conferred largely by 1,25(OH)$_2$D$_3$ (1, 7). An important additional feature of *Cyp24a1* regulation in the kidney but not in NRTCs is that this gene is controlled by each of the three hormones in a manner directionally opposite of that for *Cyp27b1*. This reciprocal regulation results in *Cyp24a1* suppression by PTH and activation by either FGF23 or 1,25(OH)$_2$D$_3$. Although we do not

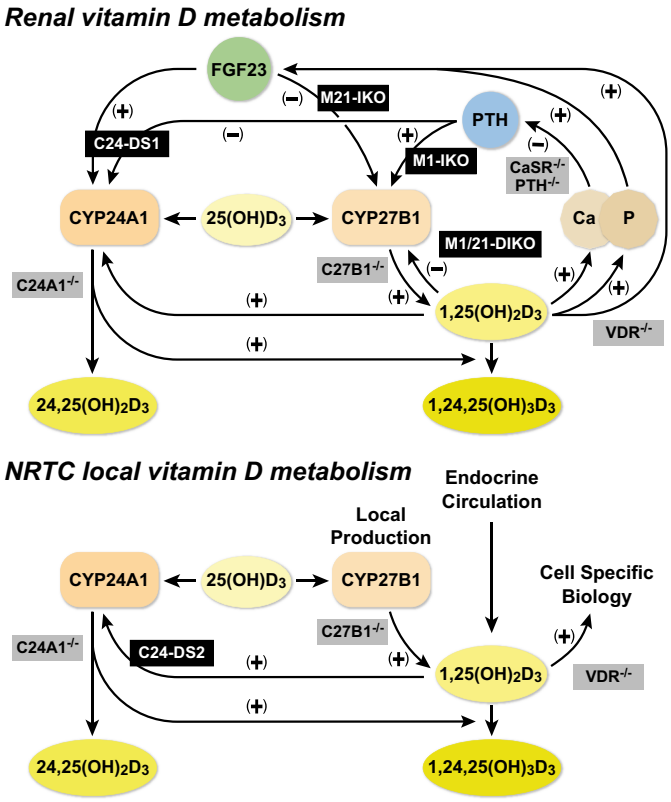

Figure 8. Vitamin D metabolism in the kidney and nonrenal tissues. *Schematic diagram* for the regulation of vitamin D metabolism and serum calcium and phosphate homeostasis in the kidney (*top*) and nonrenal target cells (NRTCs, *bottom*). Our genetic models (*black*) and previously existing models (*gray*) are overlaid on or near the pathways they disrupt. This figure was derived from our earlier publication (7).

address herein the molecular mechanisms that make this reciprocal regulation of the two genes in the kidney by these hormones possible, these separate properties of *Cyp24a1* regulation underscore distinct functional roles for the gene in the kidney *versus* NRTCs. Accordingly, *Cyp24a1* together with *Cyp27b1* operate in the former to produce and maintain stable blood levels of active $1,25(OH)_2D_3$ and to control adaptive vitamin D metabolism, as illustrated in Fig. 8. In NRTCs, however, *Cyp24a1* functions as seen in this figure specifically to modulate the steady-state level of either endocrine or locally derived $1,25(OH)_2D_3$ through dynamic control of the hormone's turnover via 24- and 23-hydroxylation, thereby likely playing a determinative role in regulating diverse biological responses.

Cyp24a1 participates in the metabolism of vitamin D through its actions to control the level of circulating $1,25(OH)_2D_3$ and to regulate its intracellular level in vitamin D target cells as well. Thus, *Cyp24a*1 is expressed in the kidney and almost ubiquitously in numerous additional tissues *in vivo*. These features underscored the need for an *in vivo* study of the regulation of *Cyp24a1*, wherein multiple target tissues and genes could be examined at a genomic level in the context of a potentially complex systemic, metabolic, and/or skeletal phenotype that we suspected might emerge as a result of altered mineral regulation. Thus, our approach involved the identification of potential regulatory regions in the *Cyp24a1* gene locus using ChIP-Seq analysis followed by CRISPR/Cas9-mediated enhancer deletion together with retention-of-function (ROF)/loss-of-function (LOF) studies in the mouse. There are multiple advantages to this *in vivo* approach, not the least of which is the ability to examine gene regulation in response to hormonal challenge in multiple tissues. Several disadvantages are also apparent, however, including the fact that the preparation of LOF/ROF deletions in mice is time-consuming and additional resolution is certain to require additional rounds of genomic deletion. A second disadvantage is that both the biological and regulatory phenotypes that emerge are likely to be highly complex, although this complexity can provide novel insight into the gene's regulation and function, as identified herein.

Our initial studies revealed a number of unexpected features of *Cyp24a1* regulation. Thus, as summarized above, we found that in concert with the well-known enhancer activity located near the *Cyp24a1* gene promoter (C24-PP1), a complex set of enhancers was also located downstream of the gene. Importantly, the more proximal subset (C24-DS1) displayed dispersed residual pCREB occupied sites, was present only in the kidney, and mediated unique regulatory properties relative to PTH and FGF23. The more distal subset (C24-DS2), on the other hand, was comprised of several clusters of VDR-binding sites that highlighted an interesting redundancy and was present in both the kidney and in NRTCs, yet appeared largely active only in nonrenal tissue types, where it increased sensitivity to the $1,25(OH)_2D_3$ hormone. These properties define a fundamental underlying genomic mechanism through which *Cyp24a1* regulation by PTH and FGF23 is restricted to the kidney, whereas the gene's regulation by $1,25(OH)_2D_3$ is mediated through differential utilization of regulatory elements present in both the kidney and in NRTCs. Interestingly, the more distal downstream VDR interactive C24-DS2 segment was identified originally by ChIP-Seq analysis in several nonrenal mouse and human cell lines (23). In these earlier studies, we also showed using mouse and human bacterial artificial chromosome clones and stable cell transfections that both regulatory regions contributed functionally to up-regulation by $1,25(OH)_2D_3$ *in vitro*, a finding that has now been duplicated in these *in vivo* studies. Our current findings will now enable us to focus on additional dissection to resolve the downstream sites of PTH *versus* FGF23 action, to confirm that pCREB is the mediator of the former hormone, and to identify the transcription factor(s) and perhaps the signaling pathway(s) that is involved in FGF23 activity at *Cyp24a1*.

The observation that *Cyp24a1* is reciprocally regulated by PTH and FGF23 in the kidney is equally important because this feature provides the distinctive homeostatic linkage between *Cyp24a1* and *Cyp27b1* that governs the regulation of circulating endocrine $1,25(OH)_2D_3$. Our previous studies and this paper show that whereas PTH induces *Cyp27b1*, it suppresses *Cyp24a1*. Similarly, whereas both FGF23 and $1,25(OH)_2D_3$ suppress *Cyp27b1*, they induce *Cyp24a1*. This reciprocal regulation results in a mechanism through which $1,25(OH)_2D_3$ can be maintained at physiological levels. Interestingly, this reciprocal regulation of *Cyp27b1* and *Cyp24a1* in the kidney is also operable for preserving blood $1,25(OH)_2D_3$ levels when either genetic, epigenetic, or pathophysiological processes cause a sustained disturbance in either *Cyp27b1* or *Cyp24a1* expres-

sion in the kidney. Thus, when the production of $1,25(OH)_2D_3$ is insufficient due to a fixed down-regulation of renal *Cyp27b1* expression, homeostatic mechanisms involving PTH and FGF23 decrease renal *Cyp24a1* expression, thereby reducing $1,25(OH)_2D_3$ turnover, which results in the preservation of circulating hormone. This leads to higher-than-expected levels of $1,25(OH)_2D_3$, prompting the hormone's characterization in patients as "inappropriately high" relative to clinical expectations. Indeed, pathophysiological reductions in *Cyp27b1* are known to arise as a result of genetic abnormalities that reduce or inhibit expression of *Cyp27b1* (alteration in expression due to SNPs, noncoding genomic deletions, or gene duplication) or reduce $1,25(OH)_2D_3$ levels due to mutations within the *Cyp27b1* gene itself (vitamin D resistance, type 1) (44–46). Each of these situations has been identified in humans and replicated in genetic mouse models as well (47). The recent generation of the M1-IKO and the M1/M21-DIKO mouse strains has revealed similar findings (7, 26). In the current studies, we show that this co-regulation is also homeostatically linked in reverse when *Cyp24a1* expression is reduced or lost, as exemplified in the C24-DS1KO mouse. Accordingly, the suppression of *Cyp24a1* expression due to the strong reduction in basal activity leads to a coordinated down-regulation of *Cyp27b1* that avoids a progressive elevation in blood $1,25(OH)_2D_3$ levels that occurs as a result of reduced turnover. Importantly, the dynamic changes in the levels of PTH and FGF23 that affect vitamin D metabolism and thus mineral homeostasis have little impact on the local expression of *Cyp24a1* or *Cyp27b1* in NRTCs and are therefore less likely to alter the biological activity of $1,25(OH)_2D_3$ in those cell types.

The concept of differential regulation also raises several questions as to why the control of *Cyp24a1* expression by $1,25(OH)_2D_3$ differs in the kidney *versus* NRTCs, where the former is modulated exclusively through the promoter-proximal region (C24-PP1), whereas the latter is regulated by both this region and the downstream distal segment (C24-DS2). The kidney represents the major endocrine source of secreted $1,25(OH)_2D_3$, so it is possible that up-regulation of *Cyp24a1* must be carefully insulated from this local production that could conflict with that of downstream PTH and/or FGF23 regulation. It is also possible that additional regulatory controls unique to the *Cyp24a1* promoter region could oppose local renal $1,25(OH)_2D_3$ action and thus blunt the up-regulatory activity of the hormone as well. This could occur because renal *Cyp24a1* is expressed largely in cells of the distal convoluted tubule, whereas *Cyp27b1* synthesis is predominantly a proximal tubule function (1). An additional question is raised as to how *Cyp24a1* promoter-proximal selectivity (at C24-PP1) can be exerted by $1,25(OH)_2D_3$ in the kidney, when VDR binding is observed in this tissue across both this region and within C24-DS2, whereas hormone activity is limited to the former. Is it possible that this downstream region contributes to renal *Cyp24a1* expression under physiological circumstances different from those tested herein? $1,25(OH)_2D_3$, on the other hand, is a strong regulator of *Cyp24a1* in NRTCs through both promoter-proximal C24-PP1 and downstream C24-DS2 regions (26). This increased sensitivity to circulating levels of $1,25(OH)_2D_3$ may underlie a dynamic mechanism for controlling the set point for intracellular $1,25(OH)_2D_3$ activity in different cell types. Perhaps more importantly, this elevated sensitivity to $1,25(OH)_2D_3$ may also provide for increased cellular resistance to potentially toxic circulating levels of renal $1,25(OH)_2D_3$ if such circumstances arise. Although these issues are all speculative, they do provide a framework for further investigation into the possible functions of *Cyp24a1* in kidney and in different NRTCs.

An investigation of the relationship between the blood concentrations of $25(OH)D_3$, $24,25(OH)_2D_3$, and $25(OH)D_3$-26,23-lactone and the level of renal *Cyp24a1* expression in a series of mutant mouse strains revealed that as *Cyp24a1* levels modestly decreased, both $24,25(OH)_2D_3$ and $25(OH)D_3$ levels tended to rise such that the $25(OH)D_3/24,25(OH)_2D_3$ ratio was maintained between 1.6 and 2. As *Cyp24a1* expression was reduced further, however, the levels of $24,25(OH)_2D_3$ and $25(OH)D_3$ diverged, resulting in an increasing ratio that reached >100. In contrast, however, a direct proportionality between the concentration of $25(OH)D_3$-26,23-lactone and the entire range of *Cyp24a1* expression was maintained, leading to ratios between $25(OH)D_3$ and $25(OH)D_3$-26,23-lactone at low levels of *Cyp24a1* expression that were much higher than 500. Although it seems counterintuitive that $24,25(OH)_2D_3$ levels should rise with declines in *Cyp24a1* expression, this differing relationship between *Cyp24a1* levels and $24,25(OH)_2D_3$ *versus* $25(OH)D_3$-26,23-lactone occurs because $24,25(OH)_2D_3$ represents the initial step in the catabolism of $25(OH)D_3$ via C24-hydroxylation, whereas the $25(OH)D_3$-26,23-lactone represents the terminal step in the catabolism of $25(OH)D_3$ via C23-hydroxylation. This was determined recently in a study where WT mice were given high doses of $24,25(OH)_2D_3$ and metabolism could be traced through all C24-hydroxylation pathway metabolites to calcioic acid, the unique final product of this pathway (48). Following *Cyp24a1* ablation, however, whereas downstream metabolites were undetectable, $24,25(OH)_2D_3$ accumulated 4-fold, highlighting the important role of CYP24A1 in the further catabolism of both $24,25(OH)_2D_3$ as well as $25(OH)D_3$. Thus, our correlative secondary analysis suggests that in the face of lowered *Cyp24a1* expression, increased $24,25(OH)_2D_3$ levels are likely due to an accumulation of uncatabolized $24,25(OH)_2D_3$, which is still being formed from $25(OH)D_3$, albeit at a slower rate than seen in WT mice. Accordingly, the peak levels of $24,25(OH)_2D_3$ that we observed in the M21-IKO mouse as well as in the current C24-DS1KO mouse likely represent the tipping point rates of $24,25(OH)_2D_3$ production relative to further degradation by CYP24A1. The direct proportionality between *Cyp24a1* expression and terminal $25(OH)D_3$-26,23-lactone levels, however, allowed several of us to conclude that the rise in the ratio of $25(OH)D_3$ to $25(OH)D_3$-26,23-lactone is a much more sensitive determinant of *Cyp24a1* expression than that of $25(OH)D_3$ to $24,25(OH)_2D_3$. Equally important in this study, whereas *Cyp24a1* was strikingly down-regulated in the kidney of each of these mouse strains, the expression of *Cyp24a1* remained unaffected in NRTCs, indicating that the enzyme in these tissues was likely not involved.

The overall profile of data obtained from these multiple strains of mice also revealed an important additional concept with regard to renal *Cyp24a1* expression. Clearly, as can be seen

in the graph in Fig. 5, the maintenance of appropriate physiological levels of $25(OH)D_3$ is fully dependent upon the normal expression and activity of renal *Cyp24a1*. Thus, as *Cyp24a1* expression becomes progressively suppressed and $24,25(OH)_2D_3$ production is eventually lost, $25(OH)D_3$ rises dramatically, leading to an increase in the ratio of the two metabolites. Because the status of each of these mice is health-adverse, characterized by hypocalcemia, hypophosphatemia, hyperparathyroidism, low levels of both FGF23 and $1,25(OH)_2D_3$, and skeletal deformities, elevated ratios appear indicative of significant pathological status due to decreased *Cyp24a1* expression and/or activity (7, 26). Thus, from a basic perspective, Fig. 5 also reveals an additional important fundamental concept that renal *Cyp24a1* modulates not only $1,25(OH)_2D_3$ but $25(OH)D_3$ levels as well. Accordingly, whereas it has been widely recognized that the hepatic synthesis of $25(OH)D_3$ via the activities of several different enzymes represents an unregulated step in the initial activation of vitamin D_3, it seems clear that the concentration of $25(OH)D_3$ in the blood is indeed actively regulated via turnover through the catabolic activity of renal *Cyp24a1*. The physiologic rationale underlying this regulation to limit $25(OH)D_3$ production levels is unclear, although it is worth noting that both the level and the potential transcriptional activity of $24,25(OH)_2D_3$ and its further metabolic degradation products is much lower than that for $25(OH)_2D_3$. Accordingly, the conversion of $25(OH)D_3$ may represent a mechanism through which the potential toxicity of $25(OH)D_3$ may be avoided when uncontrolled hepatic production is increased, by analogy with the catabolism of $1,25(OH)_2D_3$ to slightly less active $1,24,25(OH)_3D_3$. Regardless of this, it is apparent that in addition to its contribution in controlling $1,25(OH)_2D_3$ levels in the blood, renal *Cyp24a1* plays an active role in limiting and therefore maintaining physiologically appropriate levels of the $25(OH)D_3$ substrate as well.

Finally, previous studies of the *Cyp24a1* locus revealed the presence of downstream VDR clusters active in both mouse and human NRTC cell lines (23) but not in the kidney. We therefore assessed in final studies the presence of such a control mechanism in the human kidney and identified both similarities and differences. We note that whereas the downstream segments of C24-DS1 and C24-DS2 are both present in the human kidney, based upon both VDR and pCREB binding, the locations of these sites and the degree of overlap between the two appear to be much greater. Whether and how these two factors might influence each other's activity is unclear, although the actions of both PTH and FGF23 on *Cyp24a1* expression are directionally opposite each other. In any event, these observations of the human kidney suggest an increase in the complexity of the arrangement relative to the mouse and highlight the necessity in the future for examining the individual roles of each enhancer in the regulation of human *CYP24A1* expression.

In summary, we have identified a chromatin-based mechanism that mediates the selective regulation of *Cyp24a1* in the kidney and in NRTCs by PTH, FGF23, and $1,25(OH)_2D_3$. This differential regulation highlights the important contributory role that *Cyp24a1* plays in sustaining blood levels of endocrine $1,25(OH)_2D_3$ and reveals how the coordinated reciprocal regulation of both *Cyp27b1* and *Cyp24a1* contributes to this process. It also reveals the distinctive dual roles of *Cyp24a1* in the kidney to regulate the circulating levels of both $1,25(OH)_2D_3$ and $25(OH)D_3$ and in NRTCs to modulate $1,25(OH)_2D_3$ turnover and thus cellular responses in a manner that is largely independent of the hormones that control mineral metabolism. Further studies will be necessary to define the numerous individual sites of action of PTH and FGF23 in the kidneys and to understand the mechanisms that control the activation of the transcription factors involved and indeed in the case of FGF23 the identity of the factor(s) itself.

Experimental procedures

Reagents

The following reagents were used for *in vivo* injections. $1\alpha,25(OH)_2D_3$ was obtained from SAFC Global (Madison, WI), PTH(1–84) (human) was obtained from Bachem (H-1370.0100 Torrence, CA), and mouse FGF23 was from R&D Systems (FGF23, 2629-FG-025, Minneapolis, MN). Antibodies used for ChIP-Seq analysis of VDR (C-20, sc-1008, lot H1216) were purchased from Santa Cruz Biotechnology, Inc. H3K4me1 (ab8895, lot GR283603-1), H3K27ac (ab4729, lot GR3187597-1), and H3K36me3 (ab9050, lot GR273247-1) were purchased from Abcam (Cambridge, MA). pCREB (Ser-133) (06-519, lot 2762242) and H3K9ac (06-942, lot 2664263) were purchased from Millipore Corp. (Billerica, MA). Traditional genotyping PCR was completed with GoTaq (Promega, Madison, WI), and all real-time quantitative PCR (qPCR) was completed with the StepOnePlus using TaqMan for gene expression assays (Applied Biosystems, Foster City, CA). Primers were obtained from IDT (Coralville, IA).

Gene expression

Dissected tissues were frozen immediately in liquid nitrogen and stored at −80 °C. Frozen tissues were homogenized in TRIzol reagent (Life Technologies, Inc.), and RNA was isolated as per the manufacturer's instructions. 1 μg of isolated total RNA was DNase-treated, reverse-transcribed using the High Capacity cDNA Kit (Applied Biosystems), and then diluted to 100 μl with RNase/DNase-free water. qPCR was performed using primers specific to a select set of differentially expressed genes by TaqMan analyses. TaqMan Gene Expression probes (Applied Biosystems) were used for RT-PCR and are found in Table 5.

ChIP-Seq

ChIP was performed using antibodies listed under "Reagents." ChIP was performed as described previously with several modifications (7, 49). Human kidney samples were obtained from the University of Wisconsin-Madison Organ Procurement Organization with approval as recently published (26). The isolated DNA (or input DNA acquired prior to precipitation) was then validated by qPCR and further prepared for ChIP-Seq analysis. ChIP-Seq libraries were prepared as described previously (7, 50). All human data were mapped to the hg19 genome build, and mouse data were mapped to the mm9 build. All human and mouse kidney ChIP-Seq data have been deposited in the Gene Expression Omnibus (GSE129585 and GSE133025) (26).

Table 5
TaqMan assays, guide RNAs, and genotyping primers

Name	Sequence/Source	Reference
TaqMan primers		
Gapdh	Applied Biosystems	4352339E
Cyp27b1	Applied Biosystems	Mm01165918
Cyp24a1	Applied Biosystems	Mm00487244
Vdr	Applied Biosystems	Mm00437297
Primers for CRISPR		
Cyp24-DS Guide 1	TAGGGACAAGGCATCAGACG-AGG	This work
Cyp24-DS Guide 2	AGAGTCGAGCGGAAATGTGC-AGG	This work
Cyp24-DS Guide 3	GTTTATAGAATCCAGCTTGG-AGG	This work
Primers for genotyping		
Cyp24-DS1 span F	GGATGAACCAAGAAGGTGCTGTG	This work
Cyp24-DS1 span R	CTGGCGTAGTGAGGAAAACCT	This work
Cyp24-DS1 internal F	GATTTTGTTAGACGTGGCAGGG	This work
Cyp24-DS1 internal R	CTTCCTTTGGACAAGCATCGTG	This work
Cyp24-DS2 span F	ATTGCCTAACCAGCCCTCTT	This work
Cyp24-DS2 span R	TGTGGAGTGCTGGAATTTGC	This work
Cyp24-DS2 internal F	TTTAGAAGTGAGGGCTGCCA	This work
Cyp24-DS2 internal R	TTTGCTCCTGTTGACACTGC	This work

CRISPR-generated and transgenic mice

The guides used for CRISPR/Cas9-mediated genome editing were optimized for the least number of potential off-target sites and fewest sites within coding exons using the Zhang laboratory CRISPR Design tool and cross-referenced with the Liu laboratory CRISPR-DO. The guides (see Table 5) were annealed and cloned into plasmids pX330 or pX458 obtained from the Zhang laboratory via Addgene (Cambridge, MA) as described recently (51). Resulting PCR products were then transcribed *in vitro* utilizing the T7 MEGAshortscript kit (Life Technologies, Inc.) (52). The mixture of 50 ng/μl of the produced RNA guides and 40 ng/μl of Cas9 protein in injection buffer (5 mM Trizma base, 5 mM Tris-HCl, 0.1 mM EDTA, pH 7.4) was injected into the pronucleus of 1-day fertilized embryos isolated from hyperovulating female C57BL/6 mice as described previously (53). Embryos were then implanted into recipient females by the University of Wisconsin-Madison Biotechnology Genome Editing and Animal Models Core. The resultant pups were genotyped with spanning primers (Table 5), cloned, and sequenced. The top 10 predicted potential off-target sites were examined by PCR and sequencing analysis. Founder mice for DS1 (3 HETs) and DS2 (2 HETs) were retained for outbreeding and experimentation.

Animal studies

Genetically modified mice were outbred with C57BL/6 mice (Jackson Laboratory, Bar Harbor, ME) as heterozygotes. Mice were housed in high-density ventilated caging in the Animal Research Facility of the University of Wisconsin-Madison under 12-h light/dark cycles at 72° F and 45% humidity. All mice used in this study were maintained on a standard rodent chow diet (5008, Lab Diet, St. Louis, MO), aged 8–9 weeks, and then outcrossed with WT C57BL/6J mice 5 or more generations unless otherwise indicated. All experiments and tissue collections were performed in the procedure rooms in the Research Animal Facility of the University of Wisconsin-Madison. All animal studies were reviewed and approved by the Research Animal Care and Use Committee of the University of Wisconsin-Madison under Protocol A005478. Homozygous mice and littermate controls were generated by HET × HET cross and evaluated for their systemic as well as skeletal phenotypes and for both basal and hormone-regulated expression of *Cyp24a1* in the kidney and in NRTC tissues. Animals were subjected to intraperitoneal injection of 10 ng/g body weight (bw) $1,25(OH)_2D_3$ (in propylene glycol), 230 ng/g bw PTH (1–84) (in PBS), 50 ng/g bw FGF23 (in PBS + 0.1% BSA), or vehicle (EtOH or PBS). Animals were sacrificed, and tissues were collected 1 h after PTH injection, 3 h after FGF23 injection, and 6 h after $1,25(OH)_2D_3$ injection. Unless otherwise indicated, all experiments were conducted with equal numbers of males and females ($n \geq 6$). There was no difference in male and female animals unless otherwise indicated. Original data documenting the expression of *Cyp24a1* from the kidneys of M1-IKO, M21-IKO, M1/M21-DIKO, *Cyp27b1*-null, and *Cyp24a1*-null mouse strains and their individual littermate controls as well as summaries of individual phenotypes and vitamin D metabolite profiles were derived from our recently published papers (7, 26). Expression of additional genes that included *Cyp27b1* and *Vdr* was also assessed. The *Cyp24a1*-null mouse strain was a kind gift from Professor Rene St-Arnaud (Shriner's Hospital/McGill University, Montreal, Canada).

Blood chemistry

Cardiac blood was collected at the time of sacrifice. Collected blood was split into serum- or EDTA-treated plasma and incubated at room temperature for 30 min, followed by centrifugation at 6,000 rpm for 12 min (twice) to obtain serum or EDTA plasma. Serum calcium and phosphate levels were measured using the QuantiChrom™ calcium assay kit (catalog no. DICA-500, BioAssay Systems, Hayward, CA) and the QuantiChrom™ phosphate assay kit (catalog no. DIPI-500, BioAssay Systems). Circulating intact FGF23 and PTH were measured in EDTA plasma via a mouse/rat FGF23 (Intact) ELISA kit (catalog no. 60-6800, Immutopics, San Clemente, CA) and a Mouse PTH(1–84) ELISA kit (catalog no. 60-2305, Immutopics), respectively.

Quantification of serum vitamin D metabolites

Serum $25(OH)D_3$, $24,25(OH)_2D_3$, $1,25(OH)_2D_3$, and $1,24,25(OH)_3D_3$ were quantified by LC-MS/MS using previously published methods (15, 39, 40), as recently reported (7).

BMD

At 8–9 weeks of age, BMDs of the CRISPR-generated mice and their WT littermates were measured and analyzed by dual X-ray absorptiometry with a PIXImus densitometer (GE-Lunar Corp., Madison, WI) as described previously (54).

Statistical evaluation

Data were analyzed using GraphPad Prism 8 software (GraphPad Software, Inc., La Jolla, CA) and in consultation with the University of Wisconsin Statistics Department. All values are reported as mean ± S.E., and differences between group means were evaluated using one-way ANOVA, two-way ANOVA, or Student's *t* test as indicated in the figure legends.

Author contributions—J. W. P. and M. B. M. conceptualization; M. B. M., S. M. L., A. H. C., N. A. B., and M. K. investigation; J. W. P. and M. B. M. writing-original draft; N. A. B., S. M. L., M. K., and G. J. writing-review and editing; M.B.M. data curation.

Acknowledgments—We thank members of the Pike Laboratory for contributions during manuscript preparation. We also thank Kathy Krentz and the University of Wisconsin Biotechnology Center–Genome Editing and Animal Models Core for generating the CRISPR/Cas9 enhancer–deleted mice. We acknowledge the Organ Procurement Organization at the University of Wisconsin-Madison for making organ tissues available to us. We also thank Waters Corp. (through a collaboration with Queen's University) for generously providing the LC-MS/MS instrumentation used in this study.

References

1. Jones, G., Prosser, D. E., and Kaufmann, M. (2014) Cytochrome P450-mediated metabolism of vitamin D. *J. Lipid Res.* **55,** 13–31 CrossRef Medline
2. Veldurthy, V., Wei, R., Campbell, M., Lupicki, K., Dhawan, P., and Christakos, S. (2016) 25-Hydroxyvitamin D_3 24-hydroxylase: a key regulator of $1,25(OH)_2D_3$ catabolism and calcium homeostasis. *Vitam. Horm.* **100,** 137–150 CrossRef Medline
3. Veldurthy, V., Wei, R., Oz, L., Dhawan, P., Jeon, Y. H., and Christakos, S. (2016) Vitamin D, calcium homeostasis and aging. *Bone Res.* **4,** 16041 CrossRef Medline
4. Jones, G., and Tenenhouse, H. S. (2002) $1,25(OH)_2D$, the preferred substrate for CYP24. *J. Bone Miner. Res.* **17,** 179–181 CrossRef Medline
5. Jones, G., Prosser, D. E., and Kaufmann, M. (2012) 25-Hydroxyvitamin D-24-hydroxylase (CYP24A1): its important role in the degradation of vitamin D. *Arch. Biochem. Biophys.* **523,** 9–18 CrossRef Medline
6. Martineau, C., Naja, R. P., Husseini, A., Hamade, B., Kaufmann, M., Akhouayri, O., Arabian, A., Jones, G., and St-Arnaud, R. (2018) Optimal bone fracture repair requires 24R,25-dihydroxyvitamin D_3 and its effector molecule FAM57B2. *J. Clin. Invest.* **128,** 3546–3557 CrossRef Medline
7. Meyer, M. B., Benkusky, N. A., Kaufmann, M., Lee, S. M., Onal, M., Jones, G., and Pike, J. W. (2017) A kidney-specific genetic control module in mice governs endocrine regulation of the cytochrome P450 gene. *J. Biol. Chem.* **292,** 17541–17558 CrossRef Medline
8. Holick, M. F., Kleiner-Bossaller, A., Schnoes, H. K., Kasten, P. M., Boyle, I. T., and DeLuca, H. F. (1973) 1,24,25-Trihydroxyvitamin D_3: a metabolite of vitamin D_3 effective on intestine. *J. Biol. Chem.* **248,** 6691–6696 Medline
9. Chandler, J. S., Pike, J. W., and Haussler, M. R. (1982) Biosynthesis, purification and receptor binding properties of high specific radioactivity 1 alpha, 24(R),25-trihydroxy-[26,27-methyl-^{3}H]-vitamin D_3. *J. Steroid Biochem.* **16,** 303–310 CrossRef Medline
10. Wang, Y. Z., Li, H., Bruns, M. E., Uskokovic, M., Truitt, G. A., Horst, R., Reinhardt, T., and Christakos, S. (1993) Effect of 1,25,28-trihydroxyvitamin D_2 and 1,24,25-trihydroxyvitamin D_3 on intestinal calbindin-D9K mRNA and protein: is there a correlation with intestinal calcium transport? *J. Bone Miner. Res.* **8,** 1483–1490 Medline
11. St-Arnaud, R., Arabian, A., Travers, R., Barletta, F., Raval-Pandya, M., Chapin, K., Depovere, J., Mathieu, C., Christakos, S., Demay, M. B., and Glorieux, F. H. (2000) Deficient mineralization of intramembranous bone in vitamin D-24-hydroxylase-ablated mice is due to elevated 1,25-dihydroxyvitamin D and not to the absence of 24,25-dihydroxyvitamin D. *Endocrinology* **141,** 2658–2666 CrossRef Medline
12. Masuda, S., Byford, V., Arabian, A., Sakai, Y., Demay, M. B., St-Arnaud, R., and Jones, G. (2005) Altered pharmacokinetics of 1α,25-dihydroxyvitamin D3 and 25-hydroxyvitamin D3 in the blood and tissues of the 25-hydroxyvitamin D-24-hydroxylase (Cyp24a1) null mouse. *Endocrinology* **146,** 825–834 CrossRef Medline
13. Schlingmann, K. P., Kaufmann, M., Weber, S., Irwin, A., Goos, C., John, U., Misselwitz, J., Klaus, G., Kuwertz-Bröking, E., Fehrenbach, H., Wingen, A. M., Güran, T., Hoenderop, J. G., Bindels, R. J., Prosser, D. E., *et al.* (2011) Mutations in CYP24A1 and idiopathic infantile hypercalcemia. *N. Engl. J. Med.* **365,** 410–421 CrossRef Medline
14. Quarles, L. D. (2012) Skeletal secretion of FGF-23 regulates phosphate and vitamin D metabolism. *Nat. Rev. Endocrinol.* **8,** 276–286 CrossRef Medline
15. Kaufmann, M., Lee, S. M., Pike, J. W., and Jones, G. (2015) A high-calcium and phosphate rescue diet and VDR-expressing transgenes normalize serum vitamin D metabolite profiles and renal Cyp27b1 and Cyp24a1 expression in VDR null mice. *Endocrinology* **156,** 4388–4397 CrossRef Medline
16. Haussler, M. R., Baylink, D. J., Hughes, M. R., Brumbaugh, P. F., Wergedal, J. E., Shen, F. H., Nielsen, R. L., Counts, S. J., Bursac, K. M., and McCain, T. A. (1976) The assay of 1α,25-dihydroxyvitamin D3: physiologic and pathologic modulation of circulating hormone levels. *Clin. Endocrinol. (Oxf.)* **5,** 151S–165S CrossRef Medline
17. Ohyama, Y., Noshiro, M., and Okuda, K. (1991) Cloning and expression of cDNA encoding 25-hydroxyvitamin D3 24-hydroxylase. *FEBS Lett.* **278,** 195–198 CrossRef Medline
18. Ohyama, Y., Noshiro, M., Eggertsen, G., Gotoh, O., Kato, Y., Björkhem, I., and Okuda, K. (1993) Structural characterization of the gene encoding rat 25-hydroxyvitamin D_3 24-hydroxylase. *Biochemistry* **32,** 76–82 CrossRef Medline
19. Chandler, J. S., Chandler, S. K., Pike, J. W., and Haussler, M. R. (1984) 1,25-Dihydroxyvitamin D_3 induces 25-hydroxyvitamin D_3-24-hydroxylase in a cultured monkey kidney cell line (LLC-MK2) apparently deficient in the high affinity receptor for the hormone. *J. Biol. Chem.* **259,** 2214–2222 Medline
20. Ohyama, Y., Ozono, K., Uchida, M., Shinki, T., Kato, S., Suda, T., Yamamoto, O., Noshiro, M., and Kato, Y. (1994) Identification of a vitamin D-responsive element in the 5′-flanking region of the rat 25-hydroxyvitamin D_3 24-hydroxylase gene. *J. Biol. Chem.* **269,** 10545–10550 Medline
21. Ohyama, Y., Ozono, K., Uchida, M., Yoshimura, M., Shinki, T., Suda, T., and Yamamoto, O. (1996) Functional assessment of two vitamin D-responsive elements in the rat 25-hydroxyvitamin D_3 24-hydroxylase gene. *J. Biol. Chem.* **271,** 30381–30385 CrossRef Medline
22. Zierold, C., Darwish, H. M., and DeLuca, H. F. (1995) Two vitamin D response elements function in the rat 1,25-dihydroxyvitamin D 24-hydroxylase promoter. *J. Biol. Chem.* **270,** 1675–1678 CrossRef Medline
23. Meyer, M. B., Goetsch, P. D., and Pike, J. W. (2010) A downstream intergenic cluster of regulatory enhancers contributes to the induction of *CYP24A1* expression by 1α,25-dihydroxyvitamin D_3. *J. Biol. Chem.* **285,** 15599–15610 CrossRef Medline
24. Zierold, C., Reinholz, G. G., Mings, J. A., Prahl, J. M., and DeLuca, H. F. (2000) Regulation of the procine 1,25-dihydroxyvitamin D_3-24-hydroxylase (CYP24) by 1,25-dihydroxyvitamin D_3 and parathyroid hormone in AOK-B50 cells. *Arch. Biochem. Biophys.* **381,** 323–327 CrossRef Medline
25. Zierold, C., Mings, J. A., and DeLuca, H. F. (2001) Parathyroid hormone regulates 25-hydroxyvitamin D_3-24-hydroxylase mRNA by altering its stability. *Proc. Natl. Acad. Sci. U.S.A.* **98,** 13572–13576 CrossRef Medline
26. Meyer, M. B., Benkusky, N. A., Kaufmann, M., Lee, S. M., Redfield, R. R., Jones, G., and Pike, J. W. (2019) Targeted genomic deletions identify diverse enhancer functions and generate a kidney-specific, endocrine-deficient *Cyp27b1* pseudo-null mouse. *J. Biol. Chem.* **294,** 9518–9535 CrossRef Medline
27. Dhawan, P., Peng, X., Sutton, A. L., MacDonald, P. N., Croniger, C. M., Trautwein, C., Centrella, M., McCarthy, T. L., and Christakos, S. (2005) Functional cooperation between CCAAT/enhancer-binding proteins and the vitamin D receptor in regulation of 25-hydroxyvitamin D_3 24-hydroxylase. *Mol. Cell Biol.* **25,** 472–487 CrossRef Medline
28. Dhawan, P., Wieder, R., Weider, R., and Christakos, S. (2009) CCAAT enhancer-binding protein alpha is a molecular target of 1,25-dihydroxyvitamin D_3 in MCF-7 breast cancer cells. *J. Biol. Chem.* **284,** 3086–3095 CrossRef Medline
29. Raval-Pandya, M., Dhawan, P., Barletta, F., and Christakos, S. (2001) YY1 represses vitamin D receptor-mediated 25-hydroxyvitamin $D_3$24-hydroxylase transcription: relief of repression by CREB-binding protein. *Mol. Endocrinol.* **15,** 1035–1046 CrossRef Medline
30. Seth-Vollenweider, T., Joshi, S., Dhawan, P., Sif, S., and Christakos, S. (2014) Novel mechanism of negative regulation of 1,25-dihydroxyvitamin

D_3-induced 25-hydroxyvitamin D_3 24-hydroxylase (Cyp24a1) transcription: epigenetic modification involving cross-talk between protein-arginine methyltransferase 5 and the SWI/SNF complex. *J. Biol. Chem.* **289,** 33958–33970 CrossRef Medline

31. Yang, W., Friedman, P. A., Kumar, R., Omdahl, J. L., May, B. K., Siu-Caldera, M. L., Reddy, G. S., and Christakos, S. (1999) Expression of 25(OH)D3 24-hydroxylase in distal nephron: coordinate regulation by 1,25(OH)2D_3 and cAMP or PTH. *Am. J. Physiol.* **276,** E793–E805 Medline
32. Allegretto, E. A., Shevde, N., Zou, A., Howell, S. R., Boehm, M. F., Hollis, B. W., and Pike, J. W. (1995) Retinoid X receptor acts as a hormone receptor *in vivo* to induce a key metabolic enzyme for 1,25-dihydroxyvitamin D_3. *J. Biol. Chem.* **270,** 23906–23909 CrossRef Medline
33. Zierold, C., Mings, J. A., Prahl, J. M., Reinholz, G. G., and DeLuca, H. F. (2002) Protein synthesis is required for optimal induction of 25-hydroxyvitamin D_3-24-hydroxylase, osteocalcin, and osteopontin mRNA by 1,25-dihydroxyvitamin D_3. *Arch. Biochem. Biophys.* **404,** 18–24 CrossRef Medline
34. Ernst, J., and Kellis, M. (2010) Discovery and characterization of chromatin states for systematic annotation of the human genome. *Nat. Biotechnol.* **28,** 817–825 CrossRef Medline
35. Meyer, M. B., Goetsch, P. D., and Pike, J. W. (2010) Genome-wide analysis of the VDR/RXR cistrome in osteoblast cells provides new mechanistic insight into the actions of the vitamin D hormone. *J. Steroid Biochem. Mol. Biol.* **121,** 136–141 CrossRef Medline
36. Meyer, M. B., Goetsch, P. D., and Pike, J. W. (2012) VDR/RXR and TCF4/β-catenin cistromes in colonic cells of colorectal tumor origin: impact on c-FOS and c-MYC gene expression. *Mol. Endocrinol.* **26,** 37–51 CrossRef Medline
37. Ernst, J., Kheradpour, P., Mikkelsen, T. S., Shoresh, N., Ward, L. D., Epstein, C. B., Zhang, X., Wang, L., Issner, R., Coyne, M., Ku, M., Durham, T., Kellis, M., and Bernstein, B. E. (2011) Mapping and analysis of chromatin state dynamics in nine human cell types. *Nature* **473,** 43–49 CrossRef Medline
38. St-Arnaud, R. (2010) CYP24A1-deficient mice as a tool to uncover a biological activity for vitamin D metabolites hydroxylated at position 24. *J. Steroid Biochem. Mol. Biol.* **121,** 254–256 CrossRef Medline
39. Kaufmann, M., Morse, N., Molloy, B. J., Cooper, D. P., Schlingmann, K. P., Molin, A., Kottler, M. L., Gallagher, J. C., Armas, L., and Jones, G. (2017) Improved screening test for idiopathic infantile hypercalcemia confirms residual levels of serum 24,25-$(OH)_2D_3$ in affected patients. *J. Bone Miner. Res.* **32,** 1589–1596 CrossRef Medline
40. Kaufmann, M., Gallagher, J. C., Peacock, M., Schlingmann, K. P., Konrad, M., DeLuca, H. F., Sigueiro, R., Lopez, B., Mourino, A., Maestro, M., St-Arnaud, R., Finkelstein, J. S., Cooper, D. P., and Jones, G. (2014) Clinical utility of simultaneous quantitation of 25-hydroxyvitamin D and 24,25-dihydroxyvitamin D by LC-MS/MS involving derivatization with DMEQ-TAD. *J. Clin. Endocrinol. Metab.* **99,** 2567–2574 CrossRef Medline
41. Meyer, M. B., and Pike, J. W. (2013) Corepressors (NCoR and SMRT) as well as coactivators are recruited to positively regulated 1α,25-dihydroxyvitamin D_3-responsive genes. *J. Steroid Biochem. Mol. Biol.* **136,** 120–124 CrossRef Medline
42. Meyer, M. B., Benkusky, N. A., Lee, C. H., and Pike, J. W. (2014) Genomic determinants of gene regulation by 1,25-dihydroxyvitamin D_3 during osteoblast-lineage cell differentiation. *J. Biol. Chem.* **289,** 19539–19554 CrossRef Medline
43. Heikkinen, S., Väisänen, S., Pehkonen, P., Seuter, S., Benes, V., and Carlberg, C. (2011) Nuclear hormone 1α,25-dihydroxyvitamin D_3 elicits a genome-wide shift in the locations of VDR chromatin occupancy. *Nucleic Acids Res.* **39,** 9181–9193 CrossRef Medline
44. Dardenne, O., Prud'homme, J., Arabian, A., Glorieux, F. H., and St-Arnaud, R. (2001) Targeted inactivation of the 25-hydroxyvitamin D_3-1α-hydroxylase gene (CYP27B1) creates an animal model of pseudovitamin D-deficiency rickets. *Endocrinology* **142,** 3135–3141 CrossRef Medline
45. Glorieux, F. H., and St-Arnaud, R. (1998) Molecular cloning of (25-OH D)-1 alpha-hydroxylase: an approach to the understanding of vitamin D pseudo-deficiency. *Recent Prog. Horm. Res.* **53,** 341–349; discussion 350 Medline
46. Glorieux, F. H., and Pettifor, J. M. (2014) Vitamin D/dietary calcium deficiency rickets and pseudo-vitamin D deficiency rickets. *Bonekey Rep.* **3,** 524 CrossRef Medline
47. St-Arnaud, R., Messerlian, S., Moir, J. M., Omdahl, J. L., and Glorieux, F. H. (1997) The 25-hydroxyvitamin D 1-α-hydroxylase gene maps to the pseudovitamin D-deficiency rickets (PDDR) disease locus. *J. Bone Miner. Res.* **12,** 1552–1559 CrossRef Medline
48. Kaufmann, M., Martineau, C., Arabian, A., Traynor, M., St-Arnaud, R., and Jones, G. (2019) Calcioic acid: *in vivo* detection and quantification of the terminal C24-oxidation product of 25-hydroxyvitamin D. *J. Steroid Biochem. Mol. Biol.* **188,** 23–28 CrossRef Medline
49. Meyer, M. B., Zella, L. A., Nerenz, R. D., and Pike, J. W. (2007) Characterizing early events associated with the activation of target genes by 1,25-dihydroxyvitamin D_3 in mouse kidney and intestine *in vivo*. *J. Biol. Chem.* **282,** 22344–22352 CrossRef Medline
50. Meyer, M. B., Benkusky, N. A., and Pike, J. W. (2014) The RUNX2 cistrome in osteoblasts: characterization, down-regulation following differentiation, and relationship to gene expression. *J. Biol. Chem.* **289,** 16016–16031 CrossRef Medline
51. Meyer, M. B., Benkusky, N. A., and Pike, J. W. (2015) Selective distal enhancer control of the Mmp13 gene identified through clustered regularly interspaced short palindromic repeat (CRISPR) genomic deletions. *J. Biol. Chem.* **290,** 11093–11107 CrossRef Medline
52. Wang, H., Yang, H., Shivalila, C. S., Dawlaty, M. M., Cheng, A. W., Zhang, F., and Jaenisch, R. (2013) One-step generation of mice carrying mutations in multiple genes by CRISPR/Cas-mediated genome engineering. *Cell* **153,** 910–918 CrossRef Medline
53. Meyer, M., de Angelis, M. H., Wurst, W., and Kühn, R. (2010) Gene targeting by homologous recombination in mouse zygotes mediated by zinc-finger nucleases. *Proc. Natl. Acad. Sci. U.S.A.* **107,** 15022–15026 CrossRef Medline
54. Onal, M., St John, H. C., Danielson, A. L., and Pike, J. W. (2016) Deletion of the distal Tnfsf11 RL-D2 enhancer that contributes to PTH-mediated RANKL expression in osteoblast lineage cells results in a high bone mass phenotype in mice. *J. Bone Miner. Res.* **31,** 416–429 CrossRef Medline